European Journal of Medicinal Chemistry 207 (2020) 112774

Contents lists available at ScienceDirect

European Journal of Medicinal Chemistry

journal homepage: http://www.elsevier.com/locate/ejmech

Design, synthesis and biological activities of piperidine-spirooxadiazole derivatives as α7 nicotinic receptor antagonists

Han Zhang [a, 1], Xiaomeng He [a, 1], Xintong Wang [b, 1], Bo Yu [a], Siqi Zhao [a], Peili Jiao [a], Hongwei Jin [a], Zhenming Liu [a, *], KeWei Wang [c, *], Liangren Zhang [a, *], Lihe Zhang [a]

[a] State Key Laboratory of Natural and Biomimetic Drugs, School of Pharmaceutical Sciences, Peking University, Beijing, 100191, PR China
[b] Department of Molecular and Cellular Pharmacology, School of Pharmaceutical Sciences, Peking University, Beijing, 100191, PR China
[c] Department of Pharmacology, Qingdao University School of Phamacy, Qingdao, 266021, PR China

ARTICLE INFO

Article history:
Received 16 July 2020
Received in revised form
18 August 2020
Accepted 18 August 2020

Keywords:
α7 nAChR
Piperidine-spirooxadiazole derivatives
Antagonists
SAR

ABSTRACT

α: 7 nicotinic acetylcholine receptors (nAChRs) expressed in the nervous and immune systems have been suggested to play important roles in the control of inflammation. However, the lack of antagonist tools specifically inhibiting α7 nAChR impedes the validation of the channel as therapeutic target. To discover a selective α7 antagonist, we started a pharmacophore-based virtual screening and identified a piperidine-spirooxadiazole derivative **T761−0184** that acts as a α7 antagonist. A series of novel piperidine-spirooxadiazole derivatives were subsequently synthesized and evaluated using two-electrode voltage clamp (TEVC) assay in *Xenopus* oocytes. Lead compounds from two series inhibited α7 with their IC_{50} values ranging from 3.3 μM to 13.7 μM. Compound **B10** exhibited α7 selectivity over other α4β2 and α3β4 nAChR subtypes. The analysis of structure-activity relationship (SAR) provides valuable insights for further development of selective α7 nAChR antagonists.

1. Introduction

Nicotinic acetylcholine receptors (nAChRs) belong to the Cys-loop receptor superfamily, which primarily mediate signal transduction of the neurotransmitter acetylcholine (ACh) at the ganglion and neuromuscular junctions [1]. These receptors are composed of muscle-type (α1, β1, δ, γ, and ε) and neuronal (α2−α10 and β2−β4) subunits, each subunit contains a large N-terminal extracellular domain, followed by four transmembrane spans with intervening intracellular domains [2]. Functional pentameric nAChR can be subdivided in homopentamers, which are formed by five identical subunits such as α7 nAChR, or heteropentamers that result from the combination of different subunits, such as α3β4 nAChR and α4β2 nAChR [3,4]. Among them, two neuronal receptors α7 and α4β2 have been identified as primary interests from the drug discovery perspectives [5−7].

The α7 nAChR is a member of ligand-gated Ca^{2+} channel that is highly expressed in hippocampus, cortex and several subcortical limbic regions, also expressed in immune cells and endothelial cells, contributing to cognition, attention, working memory, reward pathways and inflammatory modulation [7,8]. A plentiful of evidences have supported the enhancement of α7 nAChR as potential therapeutic strategies for many diseases such as schizophrenia, Alzheimer's disease and inflammatory disorders [9−11]. However, activation of α7 nAChR may not be always beneficial. High levels of α7 nAChR expression promote cancer cell proliferation and metastasis in lung, colon, and bladder tissues [12]. Thus, selective inhibitors of α7 nAChR can inhibit cancer cell growth through reversing proangiogenic effects of nicotine [13,14]. Moreover, the inhibition of α7 nAChR has explored as potential treatment for organophosphorus nerve agent intoxication and smoking cessation [15,16].

Activation of the α7 nAChR has been widely studied, which provides us information for the design of its antagonists. The primary orthosteric ligand binding pocket for agonists and competitive antagonists is localized in the extracellular domain at the interface of two adjacent α7 subunits (loops A−C, loops D−E) [17]. ACh is an endogenous ligand that binds to the orthosteric ligand

* Corresponding authors.
E-mail addresses: zhanghan930506@163.com (H. Zhang), xhe@bjmu.edu.cn (X. He), wangxintong@bjmu.edu.cn (X. Wang), boyu@bjmu.edu.cn (B. Yu), 1811210124@bjmu.edu.cn (S. Zhao), pelly@bjmu.edu.cn (P. Jiao), jinhw@bjmu.edu.cn (H. Jin), zmliu@bjmu.edu.cn (Z. Liu), wangkw@bjmu.edu.cn (K. Wang), liangren@bjmu.edu.cn (L. Zhang), zdszlh@bjmu.edu.cn (L. Zhang).
[1] These authors contributed equally.

https://doi.org/10.1016/j.ejmech.2020.112774
0223-5234/

binding site to activate calcium influx, yielded a EC_{50} value of ~100–200 μM [18]. Over the past three decades, a variety of orthosteric agonists have been developed for the α7 nAChR as potential therapeutics, such as GTS-21, JN403 and so on [19–21]. Thereinto, several α7 nAChR selective agonists (e.g., AQW051, SSR-180711 and RG3487) have advanced to clinical trials for schizophrenia and Alzheimer's disease (Fig. 1) [22–24]. The general features of these reported α7 nAChR orthosteric agonists include: a basic fragment, which can be protonated at physiological pH and form cation-π interaction with the receptor; a hydrophobic aromatic moiety providing π-π interaction and a linker [25–27]. In addition, several allosteric modulators, e.g. AVL3288, showed different structural features compared with orthosteric modulators (Fig. 1) [28]. Therefore, development of α7 nAChR modulators has attracted increasing attention for both academic functional studies and clinical applications.

Although extensive studies have been conducted to discover selective α7 nAChR agonists, the development of α7 selective antagonists is relatively limited (Fig. 1). α-Bungarotoxin (α-BTX) and methyllycaconitine (MLA) are two frequently used α7 nAChR potent antagonists, which obtained from natural sources, also inhibit some other nAChR subtypes [20]. Besides, several α7 nAChR antagonists discovered by derivatization or structural modification of agonists, have been reported with antagonistic activities at micromolar levels (IC_{50} = 3.7–300 μM), including triazolylamide derivatives, quinoline derivatives and nicotine analogues [27,29,30]. Moreover, phenothiazine-class antipsychotics such as phenothiazine derivative and amphetamine-type stimulants amphetamine have also been reported as α7 nAChR antagonists, with IC_{50} values of 0.4 μM and 12 μM, respectively [31,32]. Overall, the reported α7 nAChR antagonists are still limited and lack of enough antagonistic activity and/or specificity. Therefore, there is an urgent need for the discovery of novel α7 nAChR antagonists, which will not only provide direct molecular tools for the pharmacological researches related to this channel, but also lead to the potential clinical therapeutic agents for related diseases.

Pharmacophore-based virtual screening approach has been an important part of many drug discovery strategies [33]. Considering that the α7 nAChR orthosteric modulators share general pharmacophoric features and many agonists already have typical pharmacophoric elements and drug-like properties. Besides, the discovery of α7 nAChR antagonists by its agonists has been reported. Therefore, we developed a pharmacophore model based on the structures of 11 reported α7 nAChR agonists and conducted virtual screening with the aid of pharmacophore-based model. As a result, piperidine-spirooxadiazole derivative **T761–0184** was discovered to be a novel α7 nAChR antagonist. To elucidate the structure-activity relationship (SAR) and discover more active compounds, a variety of **T761–0184** derivatives were further designed by modification of substituted groups at 3- and 8-position of piperidine-spirooxadiazole scaffold, especially introduction of aromatic moiety (R_1) at 3-position of the scaffold to form potential π-π stacking effect. The α7 nAChR antagonistic activities of all synthesized compounds were assessed by two-electrode voltage clamp (TEVC) assay in *Xenopus* oocytes. In addition, the antagonistic activities of the representative compound over other related nAChR subtypes were also investigated. Herein, we report the synthesis and biological investigation of these compounds, which will definitely promote the discovery of novel selective α7 nAChR antagonists [34].

2. Results and discussions

2.1. Computationally guided discovery of α7 nAChR orthosteric antagonists

In an effort to discover novel selective ligands of α7 nAChR, pharmacophore-based virtual screening approach was employed (Fig. 2). We first selected 11 reported α7 nAChR agonists according to structural diversity and rigidity as training sets (Fig. S1), and constructed a pharmacophore model based on the common features of selected compounds using HipHop program (Discovery Studio, Accelrys, Inc.). The selected model contained 1 hydrogen-bond receptor, 1 hydrophobic center and 1 positively ionized

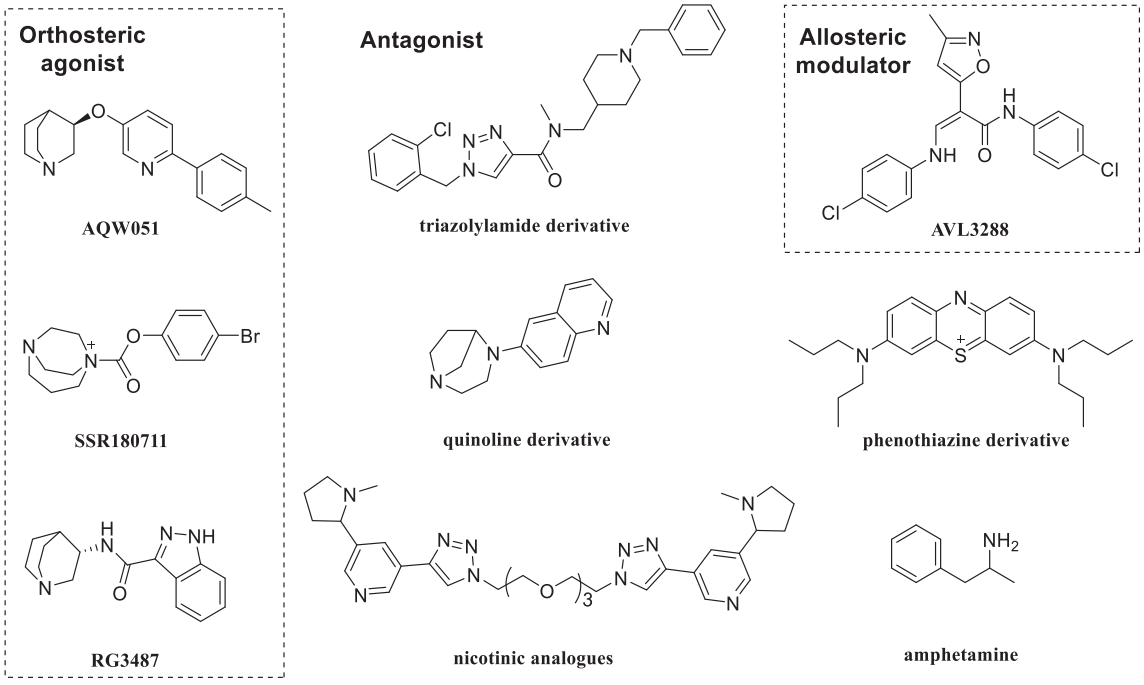

Fig. 1. Chemical structures of representative α7 nAChR modulators.

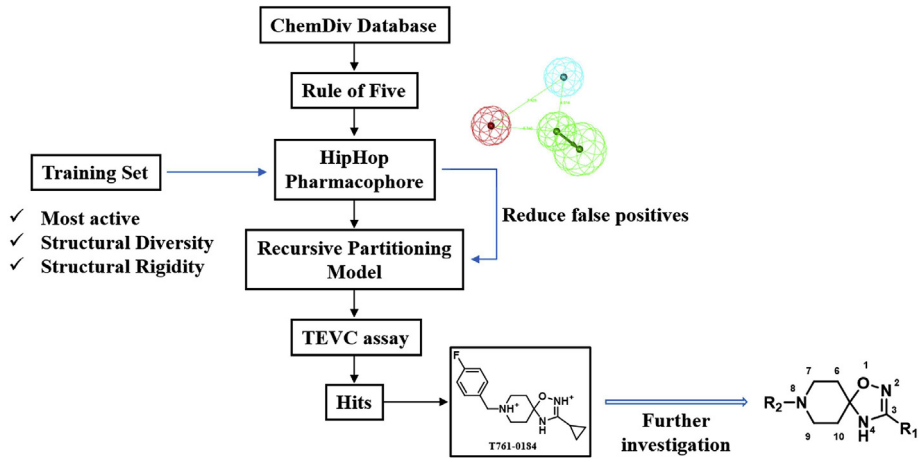

Fig. 2. Flow chart illustrating the computationally guided discovery process of α7 nAChR orthosteric antagonists.

group. Since the HipHop model produced a large number of false positive results, we established a recursive partitioning (RP) model. Then we used the afore mentioned two models to perform virtual screening of the commercial small-molecule database ChemDiv (http://www.chemdiv.org/). In order to remove unwanted structures and accelerate the process of virtual screening, the "rule of five" filter was applied before the pharmacophore-based database searching. In the end, we obtained 13 compounds for biological evaluation.

TEVC was used to evaluate the activities of these 13 compounds in *Xenopus* oocytes expressing human α7 nAChR, 10 of them showed inhibitory effects on ACh induced α7 nAChR currents (Fig. S2). For the purpose of calculating inhibition ratio, 100 μM compound was co-applied with 100 μM ACh, and the resulting currents were compared to those induced by ACh alone. Among these novel ligands for the α7 nAChR, the piperidine-spirooxadiazole derivative **T761–0184** was selected for further investigation due to its potency (Fig. 3).

To investigate the binding mode of **T761–0184** targeting orthosteric site of α7 nAChR, molecular docking studies were carried out by using Induced Fit Docking module of Schrödinger Suite (Schrödinger, LLC, New York, NY, USA). Although the three-dimensional (3D) structure of human α7 nAChR has not been solved, several structures of the extracellular region of the homologous acetylcholine binding protein (AChBP) or chimera are available, which shares 64% sequence identity and 71% similarity with native α7 nAChR [35]. So, **T761–0184** was docked to the crystal structure of human α7-AChBP chimera (PDB ID code: 3SQ6). The docking result (Fig. S3) indicated that **T761–0184** bound into the classic aromatic pocket and the piperidine-spirooxadiazole moiety could be matched well to the orthosteric binding site between two adjacent subunits, in which the piperidine *N* atom formed three cation-π interactions with residues TYR191, TRP145 and TYR184 in the form of nitrogen cations, as a novel positive charge center; The 8-position *p*-fluorobenzyl formed a π-π interaction with TRP145. Through comparing with the structural characteristics and binding mode of known α7 nAChR modulators, we found that the 3-position cyclopropyl was replaced by aromatic moiety might increase the hydrophobic interaction and the potential π-π stacking effect, suggesting us a feasible modified strategy to enhance its potency.

2.2. Chemistry

Further structural optimizations were performed on **T761–0184** to discover more active antagonists of α7 nAChR. Considering the structural similarity with known modulators, we retained the piperidine-spirooxadiazole skeleton of **T761–0184** and modified the structure mainly at its 3-position (R_1) and 8-position (R_2), which are called **Class A** and **B**, respectively (Fig. 2). The general synthetic routes for preparation of **Class A** and **B** are described in Scheme 1 and Scheme 2.

Different aryl substituted nitriles (**1a-1o**) were reacted with hydroxylamine hydrochloride via addition reaction in ethanol to afford *N*-hydroxylformamidines (**2a-2o**), which were then cyclized by reacting with *N*-benzylpiperidone using *p*-toluene sulfonic acid as catalyst in toluene to form target compounds **A1-A15** [36]. The biaryl derivatives **A16-A36** was prepared from **A7** or **A13** through Suzuki coupling reaction with substituted boric acids under the catalytic system of $Pd(PPh_3)_4$ [37].

Scheme 2 outlines the synthesis of compounds **B1**—**B15**. Treatment of piperidone with organic halides (**3a, 3b**) in the presence of

Fig. 3. Inhibition of α7 currents by **T761–0184** in two-electrode voltage clamp recordings of *Xenopus* oocytes expressing human α7 nAChRs. Representative traces of currents recorded in response to 100 μM ACh (left), 100 μM **T761–0184** (middle), and co-application of 100 μM **T761–0184** and ACh (right) using two-electrode voltage clamp.

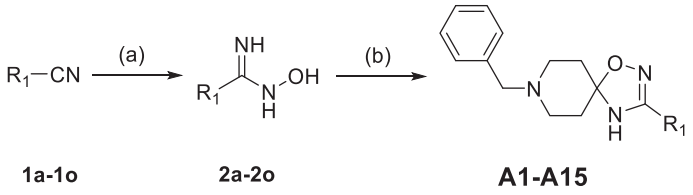

1a, 2a, A1: R_1 = cyclopropyl
1b, 2b, A2: R_1 = phenyl
1c, 2c, A3: R_1 = m-tolyl
1d, 2d, A4: R_1 = 3-fluorophenyl
1e, 2e, A5: R_1 = 4-fluorophenyl
1f, 2f, A6: R_1 = 4-chlorophenyl
1g, 2g, A7: R_1 = 4-bromophenyl
1h, 2h, A8: R_1 = 4-methoxyphenyl
1i, 2i, A9: R_1 =2,4-dimethoxyphenyl
1j, 2j, A10: R_1 = thiazol-2-yl
1k, 2k, A11: R_1 = thiophen-2-yl
1l, 2l, A12: R_1 = pyridin-2-yl
1m, 2m, A13: R_1 = 6-bromopyridin-3-yl
1n, 2n, A14: R_1 = isoquinolin-3-yl
1o, 2o, A15: R_1 = 1*H*-indazol-3-yl

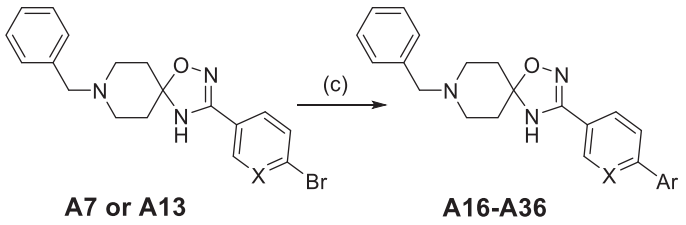

A16-A30: X = C, Ar = Substituted phenyl
A31: X = C, Ar = thiophen-2-yl
A32: X = C, Ar = pyridin-3-yl
A33: X = C, Ar = pyridin-4-yl
A34: X = C, Ar =2-methoxypyridin-4-yl
A35: X = N, Ar = 3-methoxyphenyl
A36: X = N, Ar = aniline-3-yl

Scheme 1. Synthesis of compounds **A1-A36**. Reagents and conditions: (a). $NH_2OH\bullet$ HCl, pyridine, EtOH, reflux, 2–6 h; (b) 1-Benzylpiperidin-4-one, $TsOH\bullet H_2O$, toluene, reflux, overnight; (c) Aryl boric acids, Na_2CO_3, $Pd(PPh_3)_4$, DMF, H_2O, 80–120 °C, 6–20 h.

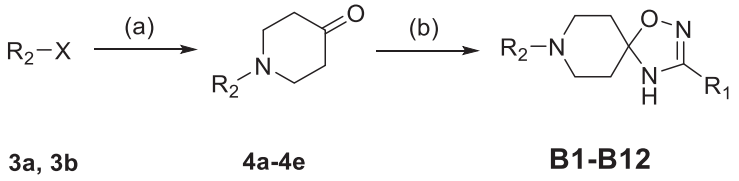

3a, 4a: R_2 = piridin-2-ylmethyl
3b, 4b: R_2 = piridin-4-ylemthyl
4c: R_2 = methyl
4d: R_2 = carbethoxy
4e: R_2 = *t*-butyloxycarbory

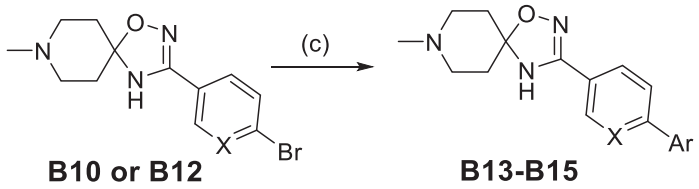

B1: R_1 = phenyl, R_2 = *t*-butyloxycarboryl
B2: R_1 = phenyl, R_2 = carbethoxy
B3: R_1 = 4-bromophenyl, R_2 =carbethoxy
B4: R_1 = phenyl, R_2 = piridin-2-ylmethyl
B5: R_1 = thiazol-2-yl, R_2 = piridin-2-ylmethyl
B6: R_1 = isoquinolin-3-yl, R_2 = piridin-2-ylmethyl
B7: R_1 = thiazol-2-yl, R_2 = piridin-4-ylemthyl
B8: R_1 = isoquinolin-3-yl, R_2 = piridin-4-ylemthyl
B9: R_1 = phenyl, R_2 = methyl
B10: R_1 = 4-bromophenyl, R_2 = methyl
B11: R_1 = thiazol-2-yl, R_2 = methyl
B12: R_1 = 6-bromopyridin-3-yl, R_2 =methyl
B13: X = C, Ar = 3-methoxyphenyl
B14: X = C, Ar = aniline-3-yl
B15: X = N, Ar = 2-methoxypyridin-4-yl

Scheme 2. Synthesis of compounds **B1**–**B15**. Reagents and conditions: (a). Piperidin-4-one, Na_2CO_3, CH_3CN, r.t., 45 min, 50 °C, 45 min, 70 °C, 2 h-overnight; (b) **2a**, **2f**, **2i**, **2l** or **2m**, $TsOH\bullet H_2O$, toluene, reflux, overnight; (c) Aryl boric acids, Na_2CO_3, $Pd(PPh_3)_4$, DMF, H_2O, 80–120 °C, 6–20 h.

sodium carbonate produced substituted piperidones (**4a, 4b**). As aforementioned, cyclization reactions were accomplished from synthesized or commercially available substituted piperidones (**4a-4e**) and *N*-hydroxyformamidines (**2a, 2f, 2i, 2l** or **2m**) to give compounds **B1**–**B12**. And the biaryl derivatives **B13**–**B15** were obtained via Suzuki coupling reaction starting from **B10** or **B12**.

2.3. Inhibitory activity and SAR

Totally, 51 compounds were synthesized and their biological activities were investigated by TEVC. The 100 μM inhibition rate of each compound was individually tested by co-application with 100 μM Ach similar with the case of **T761**–**0184**, a varied degree of antagonistic response of ACh-induced currents was observed, whereas no significant potentiation was exerted by any of the tested compounds (Tables 1–3). Of them, 24 compounds reduced more than 80% ACh-induced α7 nAChR currents increase compared with the vehicle-treated cells. Their inhibitory activities at 30 μM were further tested, 9 compounds inhibited more than 70% ACh-induced currents. The concentration-dependent response curves of several compounds that exhibited most potent inhibitory activities at the concentration of 30 μM were plotted to calculate IC_{50} values. Five compounds, i.e. **A2**, **A7**, **B9**, **B10** and **B15**, gave IC_{50} values of 3.3–13.7 μM (Fig. 4, Fig. 5).

As shown in Table 1 and Fig. 4, when the *p*-fluorobenzyl group at R_2-position of piperidine-spirooxadiazole was replaced with benzyl, compound **A1** maintained the inhibitory activity. Therefore, we retained benzyl at R_2-position and investigated the inhibitory activities of various aromatic substitution groups at R_1-position of piperidine-spirooxadiazole to discover more active compounds.

Table 1
Inhibition of α7 nAChR currents by piperidine-spirooxadiazole derivatives through modifications in R_1 on α7 nAChR currents investigated by TEVC.

Compds	R_1	100 μM Inhibition (%)[a]	30 μM Inhibition (%)[a]	IC_{50} (μM)	Agonism
A1		83.9 ± 5.0	52.2 ± 8.7		–
A2		98.2 ± 0.3	70.4 ± 2.0	13.7	–
A3		75.4 ± 4.0	–		–
A4		83.1 ± 2.0	65.9 ± 2.2		–
A5		78.3 ± 5.5	–		–
A6		90.7 ± 2.4	77.4 ± 3.8		–
A7		91.5 ± 2.0	90.8 ± 2.0	6.0	+
A8		79.6 ± 6.5	–		–
A9		79.1 ± 2.2	–		–
A10		94.5 ± 4.0	65.1 ± 2.7		–
A11		74.9 ± 1.7	–		–
A12		68.7 ± 3.3	–		–
A13		90.3 ± 2.7	63.7 ± 5.2		–
A14		91.1 ± 4.6	76.6 ± 1.8		–
A15		69.8 ± 8.1	–		–
T761–0184		83.9 ± 5.1	52.8 ± 1.6		–

"-": no activity.
"–": not measured.
[a] Percentage inhibition at test concentration, and data are the mean ± SEM from 3 to 4 determinations (n = 3–4); currents were recorded in TEVC.

Replacing cyclopropyl group at R_1-position of piperidine-spirooxadiazole with phenyl (**A2**), thiazol-2-yl (**A10**), 6-bromopyridin-3-yl (**A13**) and isoquinolin-3-yl (**A14**) resulted in higher potency than **A1**, while the other substitution groups, i.e. thiophen-2-yl (**A11**), pyridin-2-yl (**A12**) and 1*H*-indazol-3-yl (**A15**) exhibited lower inhibitory activity than **A1**. This difference might be related to the electronic density or spatial size of the aromatic moiety. Among them, phenyl substituted compound **A2** was the most potent antagonist with an IC_{50} value of 13.7 μM (Fig. 4), which lead us to further investigate the SAR of substituted phenyl derivatives. The introduction of *m*-methylphenyl (**A3**), *m*-fluorophenyl (**A4**), *p*-fluorophenyl (**A5**), *p*-methoxyphenyl (**A8**) or 2,4-dimethoxyphenyl (**A9**) substituent into the R_1-position of piperidine-spirooxadiazole decreased the inhibitory activity compared with **A2**. However, strong inhibitory activities were observed for *p*-chlorophenyl (**A6**) and *p*-bromophenyl (**A7**) substituted piperidine-spirooxadiazole derivatives, particularly **A7** showed an IC_{50} value of 6.0 μM (Fig. 4). These results demonstrated that the replacement of cyclopropyl with aromatic moieties (*p*-chlorophenyl or *p*-bromophenyl) were favorable for improving potency as we expected.

The ratio was tested as a parameter with a ratio of 100 μM ACh-activation current. "-": no agonistic activity; "+": weak agonistic effect, less than 20% of 100 μM ACh.

A1-**A15**: R_2 = benzyl; **T761–0184**: R_2 = *p*-fluorobenzyl

Since the biaryl group was a common motif among α7 orthosteric modulators, such as agonist AQW051 (Fig. 1) [24], we also replaced cyclopropyl with various biaryl groups at the R_1-position of piperidine-spirooxadiazole. As shown in Table 2, replacing the bromine atom of **A7** or **A13** with phenyl, substituted phenyl, thiophen and pyridin, decreased inhibitory activity was observed for a large proportion of resulting compounds (**A16-A19**, **A21**, **A24-A31**, **A33**, **A35**). But biaryl bearing some 3′ substitution displayed maintained or higher potency than **A1**, such as 3′-methoxy (**A20**, **A34**), 3′-hydroxy (**A22**), 3′-amino (**A23**, **A36**) and pyridin-3-yl (**A32**). These results implied that electron-donating group at 3′-position of biaryl was beneficial to increase the inhibitory activities.

The ratio was tested as a parameter with a ratio of 100 μM ACh-activation current. "-": no agonistic activity; "+": weak agonistic effect, less than 20% of 100 μM ACh.

To further study the SAR of R_2-position substituted piperidine-spirooxadiazole derivatives, we retained the substituent at R_1-

Table 2
Inhibition of α7 nAChR currents by 3-biaryl piperidine-spirooxadiazole derivatives.

Compds	R_1	100 μM Inhibition (%)[a]	30 μM Inhibition (%)[a]	IC_{50} (μM)	Agonism
A16		71.4 ± 8.4	–	–	–
A17		72.0 ± 2.6	–	–	–
A18		80.1 ± 2.7	30.0 ± 10.4	–	–
A19		26.2 ± 11.3	–	–	–
A20		95.6 ± 0.8	76.9 ± 5.1	–	–
A21		73.0 ± 9.5	–	–	–
A22		80.4 ± 2.3	59.0 ± 1.7	–	–
A23		93.5 ± 1.9	60.1 ± 3.3	–	–
A24		81.1 ± 14.5	39.5 ± 2.8	–	–
A25		67.0 ± 0.8	–	–	–
A26		34.9 ± 5.5	–	–	–
A27		42.4 ± 11.6	–	–	–
A28		52.8 ± 12.2	–	–	–
A29		40.5 ± 9.8	–	–	–
A30		36.5 ± 5.0	–	–	–
A31		71.1 ± 2.1	–	–	–
A32		81.1 ± 14.5	65.0 ± 4.4	–	–
A33		75.2 ± 2.7	–	–	–
A34		89.9 ± 2.2	54.7 ± 2.5	–	–
A35		58.2 ± 5.1	–	–	–

Table 2 (*continued*)

Compds	R_1	100 μM Inhibition (%)[a]	30 μM Inhibition (%)[a]	IC_{50} (μM)	Agonism
A36	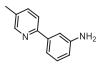	87.2 ± 3.6	61.8 ± 1.1	–	–

"-": no activity.
"–": not measured.
[a] Percentage inhibition at test concentration, and data are the mean ± SEM from 3 to 4 determinations (n = 3–4); currents were recorded in TEVC.

Table 3
Inhibition of α7 nAChR currents by piperidine-spirooxadiazole derivatives through modifications in R_2.

Compds	R_1	R_2	100 μM Inhibition (%)[a]	30 μM Inhibition (%)[a]	IC_{50} (μM)	Agonism
B1			73.5 ± 7.4	–	–	–
B2			75.1 ± 1.4	–	–	–
B3			58.1 ± 6.3	–	–	–
B4			70.2 ± 8.4	–	–	–
B5			80.0 ± 5.3	39.3 ± 10.2	–	–
B6			80.0 ± 5.2	37.9 ± 6.9	–	–
B7			18.8 ± 3.5	–	–	–
B8			58.2 ± 9.4	–	–	–
B9		– CH_3	96.7 ± 1.3	90.4 ± 0.2	4.4	–
B10		– CH_3	97.4 ± 0.3	91.8 ± 2.1	5.4	–
B11		– CH_3	87.4 ± 2.6	69.7 ± 3.6	–	–
B12		– CH_3	83.4 ± 3.8	44.1 ± 2.1	–	–
B13	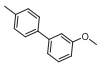	– CH_3	93.2 ± 0.5	81.3 ± 4.6	–	–
B14	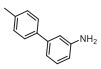	– CH_3	78.2 ± 4.4	–	–	–
B15		– CH_3	93.4 ± 0.8	86.1 ± 3.0	3.3	–

"-": no activity.
"–": not measured.
[a] Percentage inhibition at test concentration, and data are the mean ± SEM from 3 to 4 determinations (n = 3–4); currents were recorded in TEVC.

position which was favorable to the inhibitory activity and investigated the biological activities of different substituted derivatives at R_2-position (Table 3 and Fig. 5). By replacing the benzyl group at R_2-position of piperidine-spirooxadiazole with *tert*-butoxycarbonyl, ethoxycarbonyl and 2-/4-pyridylmethyl groups, compounds **B1**–**B8** were formed but decreased inhibitory activities were observed. Meanwhile, the replacement of benzyl group at R_2-position with methyl (**B9**, **B10**) resulted in improved inhibitory activities compared with corresponding R_1-substituted derivatives (**A2**, **A7**), showed IC_{50} values of 4.4 μM and 5.4 μM, respectively (Fig. 5). These probably might be the presence of electron-withdrawing groups at R_2-position of piperidine-spirooxadiazole, it was not conducive to the protonation of the piperidine *N* atom connected to it under physiological conditions, suggesting us to synthesize methyl substituted compounds (**B11**–**B15**), and compound **B15** expectedly exhibited strong inhibitory activity with an IC_{50} = 3.3 μM (Fig. 5). These results indicated that methyl substituent at R_2-position of piperidine-spirooxadiazole derivatives were favorable to the inhibitory activity.

Subsequently, we investigated the binding mode of representative compound **B10** into the orthosteric binding pocket of human α7-AChBP chimera (PDB ID code: 3SQ6) by molecular docking as

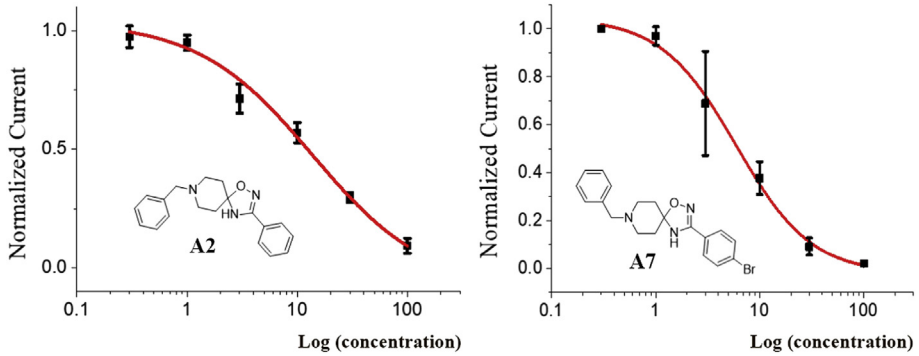

Fig. 4. Concentration-dependent inhibition of α7 AChR currents by **A2** and **A7** in TEVC assay. Data were presented as the mean ± SEM from four independent experiments (n = 4).

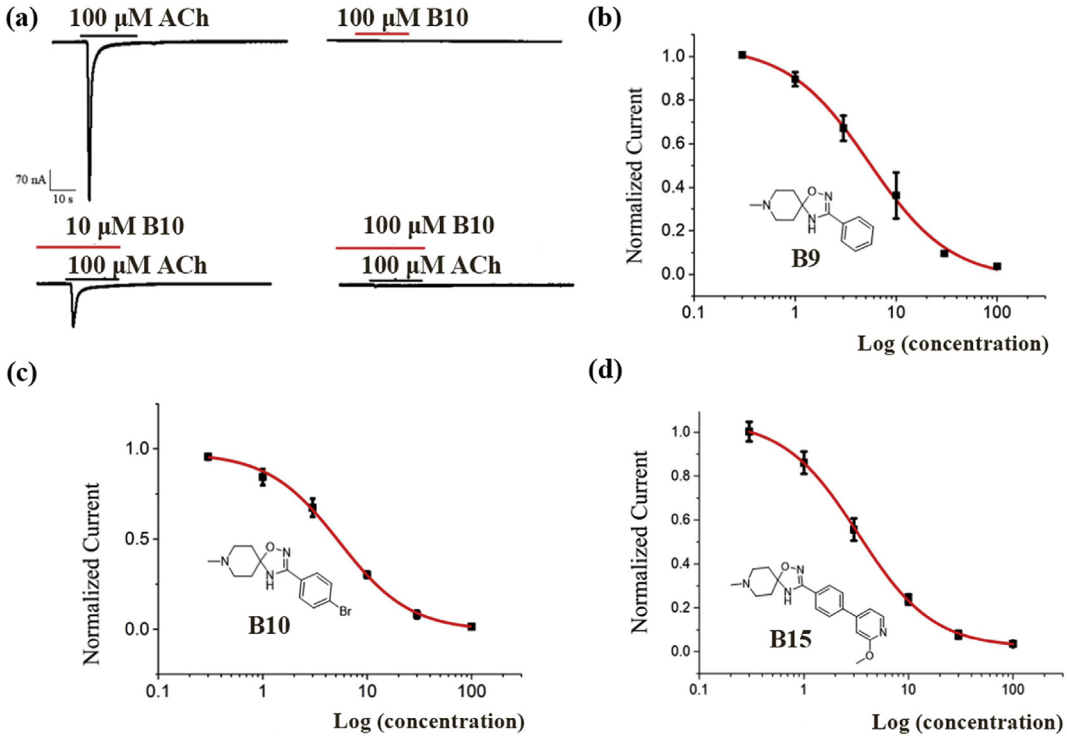

Fig. 5. Inhibition of α7 currents by **B9**, **B10** and **B15**. (a) Inhibition activity of 10 μM and 100 μM **B10** against the α7 nAChR-mediated currents. Concentration-dependent inhibition of α7 AChR currents by **B9** (b), **B10** (c) and **B15** (d). Data were presented as the mean ± SEM from four independent experiments (n = 4).

previously described in 2.1. As shown in Fig. 6, **B10** matched better to the orthosteric binding site between two adjacent subunits compared with **T761**–**0184**. Because **B10** not only maintained three cation-π interactions with residues TYR191, TRP145 and TYR184 through the piperidine *N* atom as positive charge center, but also formed a new π-π interaction with TRP53 by aromatic moiety at R_1-position of the piperidine-spirooxadiazole. This binding mode was more similar to that of known α7 AChR selective modulators, verifying the introduction of aromatic moiety increased the antagonistic activity.

Taken together, we found that aromatic moieties (*p*-bromophenyl, 3′ electron-donating groups substituted biaryl) at R_1-position and methyl at R_2-position of the piperidine-spirooxadiazole were favorable for the inhibitory activity. Our investigation illustrated that piperidine-spirooxadiazole derivatives were a series of novel potent α7 AChR antagonists, and the size and electronegativity of the substituents on the piperidine-spirooxadiazole scaffold played key roles in the inhibitory activity against α7 AchR.

*2.4. Inhibitory activities of compound **B10** on other related ligand-gated ion channels*

To evaluate the selectivity of representative compound **B10**, we examined the effects of **B10** on $\alpha4\beta2$ and $\alpha3\beta4$ nAChR by TEVC, subtypes with distributions similar to that of α7 nAChR in brain [38]. As shown in Fig. 7, the expression of $\alpha3\beta4$ and $\alpha4\beta2$ nAChR in Xenopus oocytes produced a robust current in response to 100 μM Ach. The application of **B10** (10 μM) hardly induced $\alpha3\beta4$ and $\alpha4\beta2$ nAChR currents, and the lack of effects on $\alpha3\beta4$ and $\alpha4\beta2$ nAChR were further confirmed by the co-application of **B10** with Ach, which resulted in a mild reduction of $\alpha3\beta4$ and $\alpha4\beta2$ currents by 20% and 24%, respectively. The concentration-dependent response curves of **B10** on $\alpha3\beta4$ and $\alpha4\beta2$ nAChR were plotted to calculate IC_{50} values. Compound **B10** showed only weak non-concentration-dependent inhibition on the $\alpha3\beta4$ currents, and gave an IC_{50} value of 32.0 μM on the $\alpha4\beta2$ nAChR, which displayed about 6-fold over α7 nAChR IC_{50} (5.4 μM). As a conclusion of channel selectivity

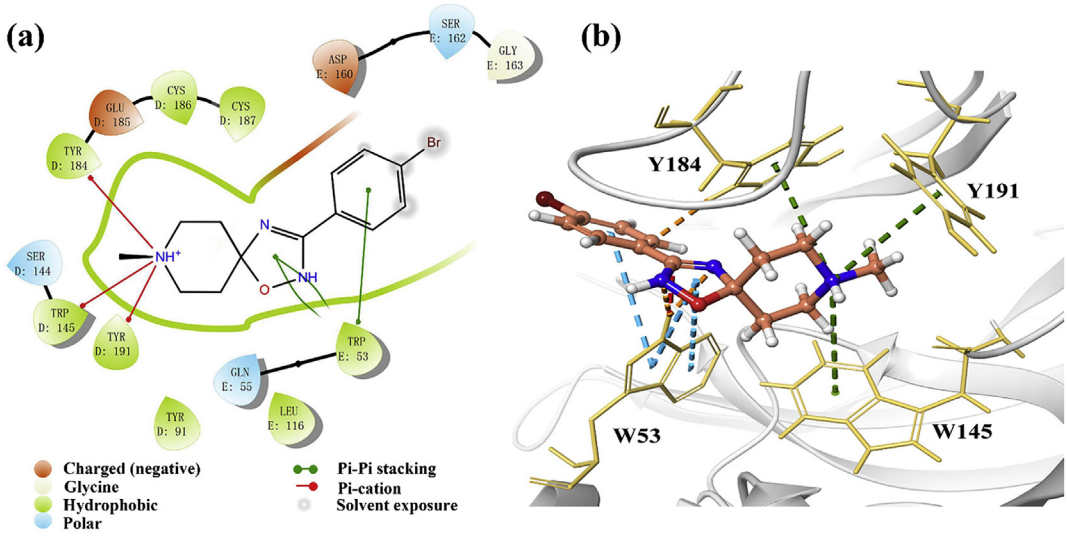

Fig. 6. 2D (a) and 3D (b) protein-ligand contacts of **B10** predicted through molecular docking. It was docked well with the orthosteric site between subunit D (including key amino acid residues W145, Y184 and Y191, etc.) and subunit E (including amino acid residues W53, Q55 and L116, etc.).

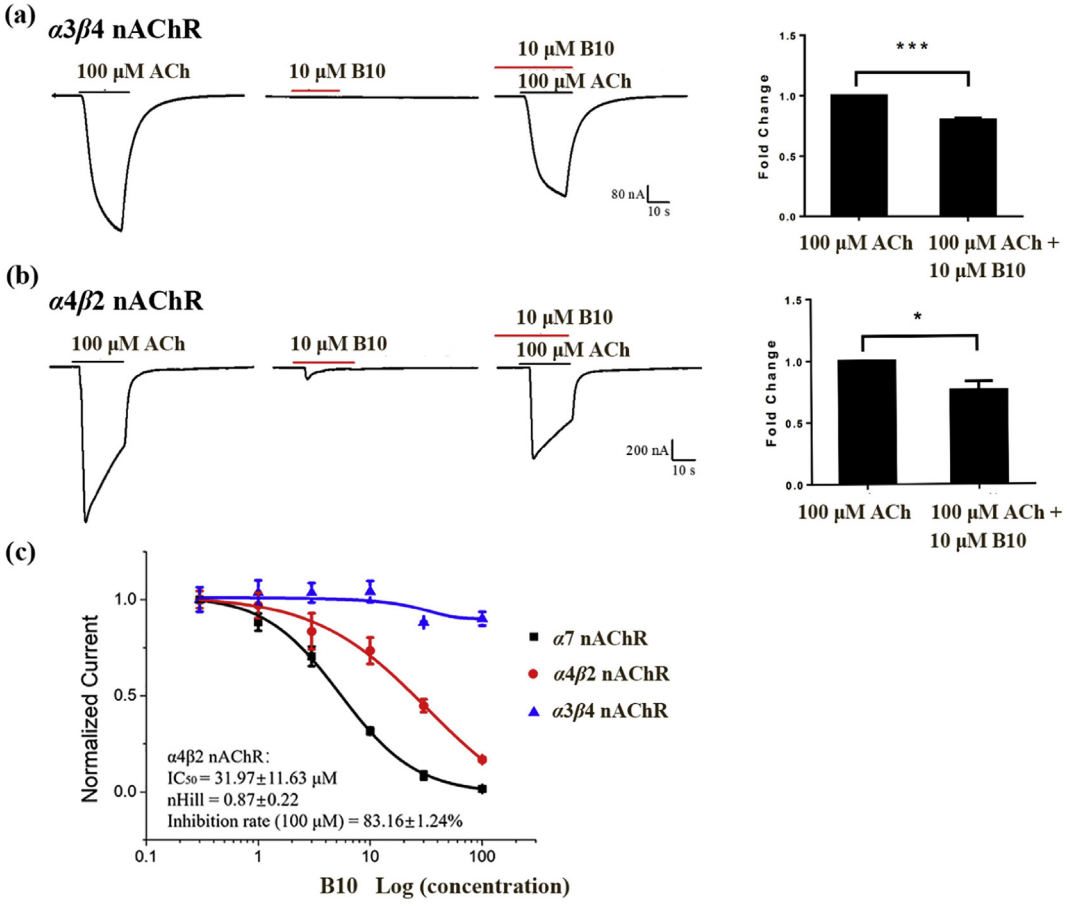

Fig. 7. Selective inhibition of α7 over α3β4 and α4β2 nAChRs by **B10** in TEVC assay. (a) Inhibition of α3β4 currents by 10 μM **B10** against. (b) Inhibition of α4β2 currents by 10 μM **B10**. (c) Summary for concentration-dependent inhibition of α7, α3β4 and α4β2 nAChR currents by **B10**. Data were presented as the mean ± SEM from four independent experiments (n = 4), and ***$P < 0.005$, *$P < 0.05$.

experiments, **B10** exhibited selectivity over $\alpha3\beta4$ and $\alpha4\beta2$ nAChR.

3. Conclusion

In this study, we discovered a potent $\alpha7$ nAChR antagonist piperidine-spirooxadiazole derivative **T761–0184** by pharmacophore-based virtual screening. For exploring the effect of 3- and 8-position moiety on the antagonistic activity and finding more potent agents, 51 **T761–0184** derivatives were designed and synthesized. All of them exhibited moderate to excellent antagonism against the $\alpha7$ nAChR, especially compounds **B9**, **B10** and **B15** (3-methyl-8-aryl) with IC_{50} values of 4.4 μM, 5.4 μM and 3.3 μM, respectively. Docking studies explained the importance of aromatic moieties at the 8-position. More importantly, **B10** showed $\alpha7$ selectivity over other $\alpha4\beta2$ and $\alpha3\beta4$ nAChR subtypes. The findings of this study provided valuable insights for the further development of selectivity $\alpha7$ nAChR antagonists.

4. Experimental section

4.1. Materials and methods

All of chemicals and solvents used were obtained from commercial sources. The solvents were dried by standard procedures. Thin layer chromatography (Silica gel GF254, Qingdao Haiyang Chemical Co., Ltd, Qingdao, China) was employed to monitor reaction process, and silica column chromatography was carried out to purify crude product (Silica gel 200–300 mesh, Shanghai Sanpont Co., Ltd, Shanghai, China). ^{1}H NMR spectra and ^{13}C NMR spectra were recorded at 400 MHz using Bruker Avance III spectrometer (Bruker CO., Switzerland) in $CDCl_3$ or DMSO-d_6 solution with tetramethylsilane as internal standard and chemical shift values were given in ppm. The NMR data was processed by software MestReNova (Ver.6.1.0, mestrelab research S.L.). The splitting peak was designed as s, singlet; d, doublet; dd, double doublet; t, triplet; m, multiplet; br, broad. The high resolution mass (HRMS) was measured on FT-MS-Bruker APEX IV mass spectrometer.

4.2. Chemical synthesis

4.2.1. General procedure for the synthesis of compounds *A1–A36*

The syntheses of compounds **A1-A36** were mainly referred to literature methods [36,37].

A mixture of hydroxylamine hydrochloride (103 mg, 1.5 mmol) and pyridine (158 mg, 2 mmol) in ethanol (5 mL) was stirred at room temperature for 15 min, followed by the addition of different aryl substituted nitriles **1a-1o** (1 mmol). The reaction mixture was refluxed for 2–6 h and the solvent was evaporated under reduced pressure. The residue was dissolved in EtOAc and washed with water three times, dried over anhydrous Na_2SO_4, filtered and concentrated under reduced pressure. The crude product was purfied by silica gel column chromatography eluting with DCM/MeOH/NH_3•H_2O (200/4/1) to afford **2a-2o**.

TsOH•H_2O (37.5 mg, 0.2 mmol) was added to a solution of **2a-2o** (1 mmol) and *N*-benzylpiperidone (285 mg, 1.5 mmol) in toluene (5 mL). The mixture was refluxed overnight. After completion, the mixture was extracted with EtOAc three times. The combined organic layers were washed with brine, dried over anhydrous Na_2SO_4, filtered and concentrated under reduced pressure. The crude product was purified by silica gel column chromatography eluting with DCM/MeOH/NH_3•H_2O (100/3/1) to afford **A1-A15**.

$Pd(PPh_3)_4$ (113 mg, 0.1 mmol) was added to a degassed mixture of **A7** or **A13** (1 mmol), substituted boric acids (2 mmol), K_2CO_3 (483 mg, 3.5 mmol) in dioxane (4 mL) and water (2 mL) under argon. The mixture was heated at 80–120 °C for 6–20 h, cooled to room temperature and extracted with EtOAc three times. The combined organic layers were washed with brine, dried over anhydrous Na_2SO_4, filtered and concentrated under reduced pressure. The crude product was purified by silica gel column chromatography eluting with PE/EtOAc/TEA (20/10/1) to afford **A16-A36**.

*4.2.1.1. 8-Benzyl-3-cyclopropyl-1-oxa-2,4,8-triazaspiro[4.5]dec-2-ene (**A1**).* White powder. Yield: 32.0%. Mp: 141–142 °C. ^{1}H NMR (400 MHz, $CDCl_3$) δ 7.31 (s, 5H), 4.08 (s, 1H), 3.53 (s, 2H), 2.69–2.36 (m, 4H), 2.13–1.86 (m, 2H), 1.85–1.68 (m, 2H), 1.59–1.50 (m, 1H), 1.01–0.83 (m, 4H). ^{13}C NMR (101 MHz, $CDCl_3$) δ 158.5, 138.1, 129.1, 128.2, 127.1, 94.8, 62.6, 50.5, 36.2, 5.9, 5.8. HRMS (ESI-TOF$^+$) *m/z* $[M+H]^+$ calcd for $C_{16}H_{22}N_3O$: 272.1763, found: 272.1766.

*4.2.1.2. 8-Benzyl-3-phenyl-1-oxa-2,4,8-triazaspiro[4.5]dec-2-ene (**A2**).* Yellow powder. Yield: 46.2%. Mp: 179–180 °C. ^{1}H NMR (400 MHz, $CDCl_3$) δ 7.68 (d, J = 7.4 Hz, 2H), 7.55–7.26 (m, 8H), 4.50 (s, 1H), 3.56 (s, 2H), 2.76–2.48 (m, 4H), 2.16–2.02 (m, 2H), 1.97–1.84 (m, 2H). ^{13}C NMR (101 MHz, $CDCl_3$) δ 155.3, 138.3, 130.7, 129.0, 128.6, 128.2, 127.1, 126.3, 125.9, 96.0, 77.2, 62.7, 50.5, 36.6. HRMS (ESI-TOF$^+$) *m/z* $[M+H]^+$ calcd for $C_{19}H_{22}N_3O$: 308.1763, found: 308.1768.

*4.2.1.3. 8-Benzyl-3-(m-tolyl)-1-oxa-2,4,8-triazaspiro[4.5]dec-2-ene (**A3**).* Yellow powder. Yield: 30.0%. Mp: 180–181 °C. ^{1}H NMR (400 MHz, $CDCl_3$) δ 7.63–7.43 (m, 2H), 7.38–7.26 (m, 7H), 4.49 (s, 1H), 3.56 (s, 2H), 2.79–2.44 (m, 4H), 2.37 (s, 3H), 2.13–1.98 (m, 2H), 1.92–1.84 (m, 2H). ^{13}C NMR (101 MHz, $CDCl_3$) δ 155.4, 138.4, 138.3, 131.5, 129.0, 128.5, 128.2, 127.1, 126.9, 125.8, 123.4, 95.9, 62.7, 50.5, 36.6, 21.3. HRMS (ESI-TOF$^+$) *m/z* $[M+H]^+$ calcd for $C_{20}H_{24}N_3O$: 322.1919, found: 322.1916.

*4.2.1.4. 8-Benzyl-3-(3-fluorophenyl)-1-oxa-2,4,8-triazaspiro[4.5]dec-2-ene (**A4**).* White powder. Yield: 24.1%. Mp: 144–145 °C. ^{1}H NMR (400 MHz, $CDCl_3$) δ 7.50–7.43 (m, 1H), 7.42–7.36 (m, 2H), 7.35–7.32 (m, 4H), 7.31–7.26 (m, 1H), 7.18–7.11 (m, 1H), 4.49 (s, 1H), 3.56 (s, 2H), 2.68–2.54 (m, 4H), 2.11–2.03 (m, 2H), 1.93–1.86 (m, 2H). ^{13}C NMR (101 MHz, $CDCl_3$) δ 164.0, 162.7 (d, J = 246.9 Hz), 154.6, 138.4, 130.5, 130.4, 129.2, 128.4, 127.2, 122.1 (d, J = 3.2 Hz), 117.8 (d, J = 21.2 Hz), 113.5 (d, J = 23.6 Hz), 96.6, 62.8, 50.6, 36.7. HRMS (ESI-TOF$^+$) *m/z* $[M+H]^+$ calcd for $C_{19}H_{21}FN_3O$: 326.1669, found: 326.1671.

*4.2.1.5. 8-Benzyl-3-(4-fluorophenyl)-1-oxa-2,4,8-triazaspiro[4.5]dec-2-ene (**A5**).* White powder. Yield: 24.8%. Mp:169–170 °C. ^{1}H NMR (400 MHz, DMSO-d_6) δ 7.72 (dd, J = 8.9, 5.5 Hz, 2H), 7.47 (s, 1H), 7.34–7.30 (m, 5H), 7.28–7.22 (m, 1H), 3.51 (s, 2H), 2.81–2.52 (m, 2H), 2.47–2.27 (m, 2H), 1.90–1.64 (m, 4H). ^{13}C NMR (101 MHz, $CDCl_3$) δ 164.12 (d, J = 251.4 Hz), 162.8, 154.5, 138.2, 129.1, 128.5, 128.4, 128.3, 127.1, 122.2, 122.2 (d, J = 3.2 Hz), 122.1, 115.9, 115.7, 96.2, 62.7, 50.5, 36.5. HRMS (ESI-TOF$^+$) *m/z* $[M+H]^+$ calcd for $C_{19}H_{21}FN_3O$: 326.1669, found: 326.1663.

*4.2.1.6. 8-Benzyl-3-(4-chlorophenyl)-1-oxa-2,4,8-triazaspiro[4.5]dec-2-ene (**A6**).* Yellow powder. Yield: 40.3%. Mp: 148–149 °C. ^{1}H NMR (400 MHz, Methanol-d_4) δ 7.70–7.62 (m, 2H), 7.49–7.42 (m, 2H), 7.39–7.30 (m, 4H), 7.30–7.23 (m, 1H), 3.58 (s, 2H), 2.83–2.69 (m, 2H), 2.56–2.43 (m, 2H), 2.01–1.84 (m, 4H). ^{13}C NMR (101 MHz, $CDCl_3$) δ 154.4, 138.3, 136.7, 129.0, 128.9, 128.2, 127.6, 127.1, 124.5, 96.4, 62.6, 50.5, 36.6. HRMS (ESI-TOF$^+$) *m/z* $[M+H]^+$ calcd for $C_{19}H_{21}N_3OCl$: 342.1373, found: 342.1371.

*4.2.1.7. 8-Benzyl-3-(4-bromophenyl)-1-oxa-2,4,8-triazaspiro[4.5]dec-2-ene (**A7**).* Yellow powder. Yield: 47.3%. Mp: 176–177 °C. ^{1}H

NMR (400 MHz, $CDCl_3$) δ 7.55 (s, 4H), 7.37–7.27 (m, 5H), 4.37 (s, 1H), 3.56 (s, 2H), 2.66–2.51 (m, 4H), 2.14–2.00 (m, 2H), 1.93–1.84 (m, 2H). ^{13}C NMR (101 MHz, $CDCl_3$) δ 154.5, 138.3, 131.9, 129.0, 128.2, 127.8, 127.1, 125.0, 124.9, 96.4, 62.6, 50.5, 36.6. HRMS (ESI-TOF$^+$) m/z $[M+H]^+$ calcd for $C_{19}H_{21}BrN_3O$: 386.0868, found: 386.0864.

*4.2.1.8. 8-Benzyl-3-(4-methoxyphenyl)-1-oxa-2,4,8-triazaspiro[4.5]dec-2-ene (**A8**).* Yellow powder. Yield: 27.7%. Mp: 150–151 °C. ^{1}H NMR (400 MHz, $CDCl_3$) δ 7.62 (d, J = 8.8 Hz, 2H), 7.38–7.26 (m, 5H), 6.91 (d, J = 8.8 Hz, 2H), 4.41 (s, 1H), 3.83 (s, 3H), 3.55 (s, 2H), 2.77–2.40 (m, 4H), 2.14–1.97 (m, 2H), 1.95–1.78 (m, 2H). ^{13}C NMR (101 MHz, $CDCl_3$) δ 161.5, 155.0, 148.6, 138.4, 129.0, 128.2, 127.9, 127.0, 118.3, 114.0, 95.7, 62.7, 55.3, 50.6, 36.5. HRMS (ESI-TOF$^+$) m/z $[M+H]^+$ calcd for $C_{20}H_{24}N_3O_2$: 338.1869, found: 338.1866.

*4.2.1.9. 8-Benzyl-3-(2,4-dimethoxyphenyl)-1-oxa-2,4,8-triazaspiro[4.5]dec-2-ene (**A9**).* Yellow powder. Yield: 29.9%. Mp: 157–158 °C. ^{1}H NMR (400 MHz, $CDCl_3$) δ 7.80 (d, J = 8.4 Hz, 1H), 7.37–7.29 (m, 4H), 6.52 (d, J = 8.4 Hz, 1H), 6.49–6.43 (m, 1H), 5.78 (s, 1H), 3.86 (s, 3H), 3.82 (s, 3H), 3.55 (s, 2H), 2.67–2.46 (m, 4H), 2.10–2.02 (m, 2H), 1.92–1.82 (m, 2H). ^{13}C NMR (101 MHz, $CDCl_3$) δ 162.7, 158.0, 154.4, 138.5, 130.6, 129.0, 128.2, 127.0, 107.1, 105.6, 98.8, 95.7, 62.7, 55.8, 55.5, 50.7, 36.2. HRMS (ESI-TOF$^+$) m/z $[M+H]^+$ calcd for $C_{21}H_{26}N_3O_3$: 368.1974, found: 368.1968.

*4.2.1.10. 8-Benzyl-3-(thiazol-2-yl)-1-oxa-2,4,8-triazaspiro[4.5]dec-2-ene (**A10**).* Yellow powder. Yield: 23.3%. ^{1}H NMR (400 MHz, $CDCl_3$) δ 7.87 (d, J = 4.0 Hz, 1H), 7.45 (d, J = 4.0 Hz, 1H), 7.41–7.27 (m, 5H), 5.38 (s, 1H), 3.56 (s, 2H), 2.71–2.43 (m, 4H), 2.17–2.03 (m, 2H), 2.00–1.88 (m, 2H). ^{13}C NMR (101 MHz, $CDCl_3$) δ 153.5, 151.6, 146.2, 143.2, 129.0, 128.3, 127.1, 121.7, 97.7, 62.6, 50.4, 36.4. HRMS (ESI-TOF$^+$) m/z $[M+H]^+$ calcd for $C_{16}H_{19}N_4OS$: 315.1280, found: 315.1283.

*4.2.1.11. 8-Benzyl-3-(thiophen-2-yl)-1-oxa-2,4,8-triazaspiro[4.5]dec-2-ene (**A11**).* White solid. Yield: 10.4%. Mp: 193–194 °C. ^{1}H NMR (400 MHz, $CDCl_3$) δ 7.57–7.24 (m, 7H), 7.06 (s, 1H), 4.65 (s, 1H), 3.56 (s, 2H), 2.75–2.45 (m, 4H), 2.19–1.98 (m, 2H), 1.97–1.81 (m, 2H). ^{13}C NMR (101 MHz, $CDCl_3$) δ 151.3, 138.2, 129.0, 128.3, 128.3, 127.8, 127.5, 127.4, 127.1, 96.4, 62.6, 50.5, 36.4. HRMS (ESI-TOF$^+$) m/z $[M+H]^+$ calcd for $C_{17}H_{20}N_3OS$: 314.1327, found: 314.1334.

*4.2.1.12. 8-Benzyl-3-(pyridin-2-yl)-1-oxa-2,4,8-triazaspiro[4.5]dec-2-ene (**A12**).* Yellow powder. Yield: 22.2%. Mp: 142–143 °C. ^{1}H NMR (400 MHz, $CDCl_3$) δ 8.56 (d, J = 5.0 Hz, 1H), 7.95 (d, J = 8.0 Hz, 1H), 7.73 (t, J = 7.8 Hz, 1H), 7.34–7.25 (m, 6H), 5.67 (s, 1H), 3.55 (s, 2H), 2.71–2.53 (m, 4H), 2.12–2.04 (m, 2H), 1.95–1.87 (m, 2H). ^{13}C NMR (101 MHz, $CDCl_3$) δ 155.4, 148.9, 145.2, 138.3, 136.6, 129.0, 128.2, 127.1, 124.9, 121.9, 96.8, 62.7, 50.5, 36.5. HRMS (ESI-TOF$^+$) m/z $[M+H]^+$ calcd for $C_{18}H_{21}N_4O$: 309.1715, found: 309.1714.

*4.2.1.13. 8-Benzyl-3-(6-bromopyridin-3-yl)-1-oxa-2,4,8-triazaspiro[4.5]dec-2-ene (**A13**).* Yellow powder. Yield: 38.8%. Mp: 169–170 °C. ^{1}H NMR (400 MHz, $CDCl_3$) δ 8.60 (s, 1H), 7.88 (d, J = 8.0 Hz, 1H), 7.53 (d, J = 8.4 Hz, 1H), 7.41–7.27 (m, 5H), 4.55 (s, 1H), 3.56 (s, 2H), 2.70–2.52 (m, 4H), 2.09–2.02 (m, 2H), 1.94–1.88 (m, 2H). ^{13}C NMR (101 MHz, $CDCl_3$) δ 152.4, 147.4, 144.1, 138.1, 136.0, 129.0, 128.3, 128.2, 127.1, 121.7, 97.1, 62.6, 50.3, 36.5. HRMS (ESI-TOF$^+$) m/z $[M+H]^+$ calcd for $C_{18}H_{20}BrN_4O$: 387.0820, found: 387.0817.

*4.2.1.14. 8-Benzyl-3-(isoquinolin-3-yl)-1-oxa-2,4,8-triazaspiro[4.5]dec-2-ene (**A14**).* Yellow powder. Yield: 26.2%. Mp: 140–141 °C. ^{1}H NMR (400 MHz, $CDCl_3$) δ 9.19 (s, 1H), 8.37 (s, 1H), 7.99 (d, J = 8.0 Hz, 1H), 7.88 (d, J = 8.0 Hz, 1H), 7.74 (t, J = 7.6 Hz, 1H), 7.66 (t, J = 8.0 Hz, 1H), 7.37–7.26 (m, 5H), 5.78 (s, 1H), 3.57 (s, 2H), 2.77–2.46 (m, 4H), 2.19–2.07 (m, 2H), 2.00–1.91 (m, 2H). ^{13}C NMR (101 MHz, $CDCl_3$) δ 155.8, 151.9, 138.5, 135.6, 138.4, 131.1, 129.0, 128.5, 128.2, 127.6, 127.4, 127.0, 119.1, 106.5, 96.6, 62.7, 50.6, 36.5. HRMS (ESI-TOF$^+$) m/z $[M+H]^+$ calcd for $C_{22}H_{23}N_4O$: 359.1872, found: 359.1867.

*4.2.1.15. 8-Benzyl-3-(1H-indazol-3-yl)-1-oxa-2,4,8-triazaspiro[4.5]dec-2-ene (**A15**).* Yellow powder. Yield: 45.0%. Mp: 150–151 °C. ^{1}H NMR (400 MHz, $CDCl_3$) δ 11.00 (brs, 1H), 8.19 (d, J = 8.2 Hz, 1H), 7.45 (t, J = 8.9 Hz, 2H), 7.37–7.27 (m, 6H), 5.36 (s, 1H), 3.58 (s, 2H), 2.74–2.57 (m, 4H), 2.17–2.07 (m, 2H), 2.01–1.93 (m, 2H). ^{13}C NMR (101 MHz, $CDCl_3$) δ 151.5, 141.0, 138.0, 133.5, 129.1, 128.3, 127.7, 127.2, 122.6, 122.3, 120.7, 109.8, 95.5, 62.7, 50.6, 36.3. HRMS (ESI-TOF$^+$) m/z $[M+H]^+$ calcd for $C_{20}H_{22}N_5O$: 348.1811, found: 348.1815.

*4.2.1.16. 3-([1,1′-Biphenyl]-4-yl)-8-benzyl-1-oxa-2,4,8-triazaspiro[4.5]dec-2-ene (**A16**).* Yellow powder. Yield: 66.7%. Mp: 195–196 °C. ^{1}H NMR (400 MHz, $CDCl_3$) δ 7.75 (m, 2H), 7.70–7.42 (m, 8H), 7.37–7.31 (m, 4H), 4.61 (s, 1H), 3.60 (s, 2H), 2.83–2.53 (m, 4H), 2.18–2.03 (m, 2H), 2.01–1.89 (m, 2H). ^{13}C NMR (101 MHz, $CDCl_3$) δ 155.1, 143.5, 140.0, 132.1, 129.2, 128.9, 128.3, 127.9, 127.3, 127.2, 127.0, 126.8, 124.7, 95.9, 62.5, 50.4, 36.3. HRMS (ESI-TOF$^+$) m/z $[M+H]^+$ calcd for $C_{25}H_{26}N_3O$: 384.2076, found: 384.2072.

*4.2.1.17. 8-Benzyl-3-(2′-methyl-[1,1′-biphenyl]-4-yl)-1-oxa-2,4,8-triazaspiro[4.5]dec-2-ene (**A17**).* Yellow powder. Yield: 32.3%%. Mp: 199–200 °C. ^{1}H NMR (400 MHz, $CDCl_3$) δ 7.72 (d, J = 8.4 Hz, 2H), 7.40–7.27 (m, 7H), 7.26–7.12 (m, 4H), 4.64 (s, 1H), 3.55 (s, 2H), 2.79–2.50 (m, 4H), 2.24 (s, 3H), 2.10–2.03 (m, 2H), 1.97–1.86 (m, 2H). ^{13}C NMR (101 MHz, $CDCl_3$) δ 155.2, 144.5, 140.8, 138.3, 135.2, 130.4, 129.5, 129.5, 129.0, 128.3, 127.7, 127.1, 126.1, 125.9, 124.4, 96.1, 62.7, 50.6, 36.6, 20.4. HRMS (ESI-TOF$^+$) m/z $[M+H]^+$ calcd for $C_{26}H_{28}N_3O$: 398.2232, found: 398.2230.

*4.2.1.18. 8-Benzyl-3-(3′-methyl-[1,1′-biphenyl]-4-yl)-1-oxa-2,4,8-triazaspiro[4.5]dec-2-ene (**A18**).* White powder. Yield: 38.7%. Mp: 186–187 °C. ^{1}H NMR (400 MHz, $CDCl_3$) δ 7.74 (d, J = 8.1 Hz, 2H), 7.62 (d, J = 8.1 Hz, 2H), 7.45–7.27 (m, 8H), 7.20 (d, J = 7.2 Hz, 1H), 4.58 (s, 1H), 3.58 (s, 2H), 2.86–2.53 (m, 4H), 2.43 (s, 3H), 2.13–2.05 (m, 2H), 1.97–1.86 (m, 2H). ^{13}C NMR (101 MHz, $CDCl_3$) δ 155.1, 143.6, 140.0, 138.5, 138.3, 129.0, 128.8, 128.6, 128.3, 127.8, 127.3, 127.1, 126.7, 124.6, 124.2, 96.1, 62.7, 50.5, 36.6, 21.5. HRMS (ESI-TOF$^+$) m/z $[M+H]^+$ calcd for $C_{26}H_{28}N_3O$: 398.2232, found: 398.2232.

*4.2.1.19. 8-Benzyl-3-(3′-isopropyl-[1,1′-biphenyl]-4-yl)-1-oxa-2,4,8-triazaspiro[4.5]dec-2-ene (**A19**).* White powder. Yield: 74.8%. Mp: 148–149 °C. ^{1}H NMR (400 MHz, $CDCl_3$) δ 7.75 (d, J = 8.4 Hz, 2H), 7.63 (d, J = 8.4 Hz, 2H), 7.45 (s, 1H), 7.44–7.37 (m, 2H), 7.37–7.26 (m, 6H), 4.57 (s, 1H), 3.58 (s, 2H), 2.99 (m, J = 6.9 Hz, 1H), 2.75–2.55 (m, 4H), 2.11–2.04 (m, 2H), 1.98–1.88 (m, 2H), 1.32 (s, 3H), 1.30 (s, 3H). ^{13}C NMR (101 MHz, $CDCl_3$) δ 155.1, 149.6, 143.8, 140.0, 138.2, 132.0, 129.0, 128.9, 128.3, 127.3, 127.1, 126.7, 126.0, 125.3, 124.6, 96.1, 62.6, 50.5, 36.5, 34.2, 24.0. HRMS (ESI-TOF$^+$) m/z $[M+H]^+$ calcd for $C_{28}H_{32}N_3O$: 426.2545, found: 426.2543.

*4.2.1.20. 8-Benzyl-3-(3′-methoxy-[1,1′-biphenyl]-4-yl)-1-oxa-2,4,8-triazaspiro[4.5]dec-2-ene (**A20**).* Yellow powder. Yield: 15.6%. ^{1}H NMR (400 MHz, $CDCl_3$) δ 7.77–7.69 (m, 2H), 7.57 (dd, J = 18.8, 8.4 Hz, 4H), 7.42–7.32 (m, 4H), 7.31–7.27 (m, 1H), 6.99 (d, J = 8.4 Hz, 2H), 4.54 (s, 1H), 3.86 (s, 3H), 3.62 (s, 2H), 2.81–2.57 (m, 4H), 2.14–2.06 (m, 2H), 2.00–1.94 (m, 2H). ^{13}C NMR (101 MHz, $CDCl_3$) δ 159.6, 155.2, 143.1, 132.4, 129.2, 128.3, 128.1, 127.4, 126.8, 126.7, 123.9, 119.5, 114.3, 95.7, 62.5, 55.3, 50.5, 36.3. HRMS (ESI-TOF$^+$) m/z $[M+H]^+$ calcd for $C_{26}H_{28}N_3O_2$: 414.2182, found: 414.2180.

*4.2.1.21. 8-Benzyl-3-(3′,5′-dimethoxy-[1,1′-biphenyl]-4-yl)-1-oxa-2,4,8-triazaspiro[4.5]dec-2-ene (**A21**).* Yellow powder. Yield: 20%. Mp: 158−159 °C. ^{1}H NMR (400 MHz, $CDCl_3$) δ 7.84−7.69 (m, 2H), 7.66−7.56 (m, 2H), 7.44−7.27 (m, 5H), 6.72 (s, 2H), 6.49 (s, 1H), 4.52 (s, 1H), 3.85 (s, 6H), 3.57 (s, 2H), 2.79−2.47 (m, 4H), 2.16−2.01 (m, 2H), 1.98−1.83 (m, 2H). ^{13}C NMR (101 MHz, $CDCl_3$) δ 161.1, 155.1, 143.4, 143.4, 142.2, 138.3, 129.0, 128.2, 127.3, 127.1, 126.7, 125.0, 105.4, 99.7, 96.2, 62.7, 55.4, 50.5, 36.6. HRMS (ESI-TOF$^+$) m/z $[M+H]^+$ calcd for $C_{27}H_{30}N_3O_3$: 444.2287, found: 444.2290.

*4.2.1.22. 4′-(8-Benzyl-1-oxa-2,4,8-triazaspiro[4.5]dec-2-en-3-yl)-[1,1′-biphenyl]-3-ol (**A22**).* White powder. Yield: 96.2%. Mp: 194−195 °C. ^{1}H NMR (400 MHz, $CDCl_3$) δ 7.65 (d, J = 7.8 Hz, 2H), 7.49 (d, J = 7.8 Hz, 2H), 7.43−7.27 (m, 6H), 7.14−6.97 (m, 2H), 6.89 (d, J = 7.4 Hz, 1H), 4.88 (s, 1H), 3.68 (s, 2H), 3.09−2.39 (m, 4H), 2.22−1.84 (m, 4H). ^{13}C NMR (101 MHz, Methanol-d_4) δ 157.3, 156.1, 143.6, 141.3, 129.7, 129.7, 128.3, 127.7, 127.0, 126.6, 124.1, 118.2, 114.7, 113.6, 95.1, 62.2, 50.0, 35.1. HRMS (ESI-TOF$^+$) m/z $[M+H]^+$ calcd for $C_{25}H_{26}N_3O_2$: 400.2025, found: 400.2025.

*4.2.1.23. 4′-(8-Benzyl-1-oxa-2,4,8-triazaspiro[4.5]dec-2-en-3-yl)-[1,1′-biphenyl]-3-amine (**A23**).* White powder. Yield: 30.1%. Mp: 184−185 °C. ^{1}H NMR (400 MHz, $CDCl_3$) δ 7.72 (d, J = 8.0 Hz, 2H), 7.59 (d, J = 8.0 Hz, 2H), 7.41−7.27 (m, 5H), 7.24−7.16 (m, 1H), 6.98 (d, J = 7.6 Hz, 1H), 6.90 (s, 1H), 6.70 (d, J = 7.6 Hz, 1H), 4.57 (s, 1H), 3.77 (brs, 2H), 3.58 (s, 2H), 2.72−2.54 (m, 4H), 1.97−1.87 (m, 2H), 1.97−1.87 (m, 2H). ^{13}C NMR (101 MHz, $CDCl_3$) δ 155.2, 146.8, 143.7, 141.2, 138.1, 129.8, 129.1, 128.3, 127.2, 127.1, 126.6, 124.6, 117.5, 114.6, 113.6, 96.0, 62.6, 50.5, 36.5, 29.7. HRMS (ESI-TOF$^+$) m/z $[M+H]^+$ calcd for $C_{25}H_{27}N_4O$: 399.2185, found: 399.2183.

*4.2.1.24. 4′-(8-Benzyl-1-oxa-2,4,8-triazaspiro[4.5]dec-2-en-3-yl)-N,N-dimethyl-[1,1′-biphenyl]-3-amine (**A24**).* Yellow powder. Yield: 45.5%. Mp: 174−175 °C. ^{1}H NMR (400 MHz, $CDCl_3$) δ 7.74 (d, J = 8.3 Hz, 2H), 7.63 (d, J = 8.3 Hz, 2H), 7.46−7.26 (m, 6H), 7.00−6.87 (m, 2H), 6.77 (dd, J = 8.3, 2.0 Hz, 1H), 4.58 (s, 1H), 3.57 (s, 2H), 3.01 (s, 6H), 2.74−2.46 (m, 4H), 2.11−2.05 (m, 2H), 1.96−1.86 (m, 2H). ^{13}C NMR (101 MHz, $CDCl_3$) δ 155.2, 150.9, 144.5, 141.0, 138.3, 129.5, 129.1, 128.3, 127.5, 127.1, 126.6124.5, 115.5, 112.1, 111.2, 96.1, 62.7, 50.5, 40.6, 36.6. HRMS (ESI-TOF$^+$) m/z $[M+H]^+$ calcd for $C_{27}H_{31}N_4O$: 427.2484, found: 427.2491.

*4.2.1.25. 8-Benzyl-3-(3′-(trifluoromethyl)-[1,1′-biphenyl]-4-yl)-1-oxa-2,4,8-triazaspiro[4.5]dec-2-ene (**A25**).* Yellow powder. Yield: 38.5%. Mp: 193−194 °C. ^{1}H NMR (400 MHz, $CDCl_3$) δ 7.89−7.67 (m, 4H), 7.67−7.51 (m, 4H), 7.33 (d, J = 23.2 Hz, 5H), 4.56 (s, 1H), 3.62 (s, 2H), 2.78−2.53 (m, 4H), 2.15−2.05 (m, 2H), 2.03−1.94 (m, 2H). ^{13}C NMR (101 MHz, $CDCl_3$) δ 154.9, 141.9, 140.8, 131.3 (q, J = 32.3 Hz), 130.3, 129.4, 129.2, 128.4, 127.4, 126.9, 124.1 (q, J = 284.8 Hz), 124.6, 124.6, 124.5, 123.8, 123.8, 96.0, 62.5, 50.4, 36.2. HRMS (ESI-TOF$^+$) m/z $[M+H]^+$ calcd for $C_{26}H_{25}F_3N_3O$: 452.1950, found: 452.1941.

*4.2.1.26. 8-Benzyl-3-(4′-methyl-[1,1′-biphenyl]-4-yl)-1-oxa-2,4,8-triazaspiro[4.5]dec-2-ene (**A26**).* Yellow powder. Yield: 19.2%. Mp: 213−214 °C. ^{1}H NMR (400 MHz, $CDCl_3$) δ 7.73 (d, J = 8.2 Hz, 2H), 7.62 (d, J = 8.0 Hz, 2H), 7.51 (d, J = 7.8 Hz, 2H), 7.39−7.26 (m, 7H), 4.48 (s, 1H), 3.57 (s, 2H), 2.73−2.53 (m, 4H), 2.40 (s, 3H), 2.15−2.05 (m, 2H), 1.96−1.87 (m, 2H). ^{13}C NMR (101 MHz, $CDCl_3$) δ 155.1, 143.4, 138.2, 137.8, 137.1, 129.6, 129.1, 128.3, 127.1, 127.0, 126.9, 126.7, 96.0, 62.7, 50.5, 36.5, 21.1. HRMS (ESI-TOF$^+$) m/z $[M+H]^+$ calcd for $C_{26}H_{28}N_3O$: 398.2232, found: 398.2225.

*4.2.1.27. 8-Benzyl-3-(4′-fluoro-[1,1′-biphenyl]-4-yl)-1-oxa-2,4,8-triazaspiro[4.5]dec-2-ene (**A27**).* Yellow powder. Yield: 33.3%. Mp: 203−204 °C. ^{1}H NMR (400 MHz, $CDCl_3$) δ 7.81−7.71 (m, 2H), 7.59−7.53 (m, 4H), 7.42−7.28 (m, 5H), 7.14 (t, J = 8.2 Hz, 2H), 4.62 (s, 1H), 3.58 (s, 2H), 2.78−2.49 (m, 4H), 2.12−2.03 (m, 2H), 1.96−1.88 (m, 2H). 13C NMR (101 MHz, $CDCl_3$) δ162.8 (d, J = 247.8 Hz),155.0, 142.4, 138.0, 132.0 (d, J = 10.1 Hz), 129.1, 128.7, 128.6, 128.3, 127.1, 126.8, 124.7, 115.8 (d, J = 21.5 Hz), 96.1, 62.6, 50.5, 36.5. HRMS (ESI-TOF$^+$) m/z $[M+H]^+$ calcd for $C_{25}H_{25}FN_3O$: 402.1982, found: 402.1978.

*4.2.1.28. 8-Benzyl-3-(4′-chloro-[1,1′-biphenyl]-4-yl)-1-oxa-2,4,8-triazaspiro[4.5]dec-2-ene (**A28**).* Yellow powder. Yield: 24.6%. Mp: 228−229 °C. ^{1}H NMR (400 MHz, $CDCl_3$) δ 7.75 (d, J = 8.4 Hz, 2H), 7.59 (d, J = 8.4 Hz, 2H), 7.53 (d, J = 8.4 Hz, 2H), 7.42 (d, J = 8.4 Hz, 2H), 7.34 (d, J = 4.4 Hz, 5H), 4.50 (s, 1H), 3.58 (s, 2H), 2.74−2.54 (m, 4H), 2.13−2.04 (m, 2H), 1.98−1.88 (m, 2H). ^{13}C NMR (101 MHz, $CDCl_3$) δ 155.0, 142.2, 138.4, 138.1, 134.1, 129.1, 129.1, 128.3, 127.2, 127.1, 126.8, 125.0, 96.1, 62.6, 50.5, 36.5. HRMS (ESI-TOF$^+$) m/z $[M+H]^+$ calcd for $C_{25}H_{25}ClN_3O$: 418.1686, found: 418.1685.

*4.2.1.29. 8-Benzyl-3-(4′-methoxy-[1,1′-biphenyl]-4-yl)-1-oxa-2,4,8-triazaspiro[4.5]dec-2-ene (**A29**).* Yellow powder. Yield: 70.7%. Mp: 230−231 °C. ^{1}H NMR (400 MHz, $CDCl_3$) δ 7.72 (d, J = 8.4 Hz, 2H), 7.57 (dd, J = 17.6, 8.4 Hz, 4H), 7.39−7.26 (m, 5H), 6.99 (d, J = 8.4 Hz, 2H), 4.54 (s, 1H), 3.86 (s, 3H), 3.57 (s, 2H), 2.78−2.48 (m, 4H), 2.14−2.02 (m, 2H), 1.97−1.86 (m, 2H). ^{13}C NMR (101 MHz, $CDCl_3$) δ 159.6, 155.2, 143.0, 138.2, 132.4, 129.1, 128.3, 128.1, 127.1, 126.7, 126.7, 124.0, 114.3, 96.0, 62.7, 55.3, 50.5, 36.5. HRMS (ESI-TOF$^+$) m/z $[M+H]^+$ calcd for $C_{26}H_{28}N_3O_2$: 414.2182, found: 414.2177.

*4.2.1.30. 8-Benzyl-3-(4′-(trifluoromethyl)-1,2-dihydro-[1,1′-biphenyl]-4-yl)-1-oxa-2,4,8-triazaspiro [4.5]dec-2-ene (**A30**).* Yellow powder. Yield: 34.0%. Mp: 226−227 °C. ^{1}H NMR (400 MHz, $CDCl_3$) δ 7.79 (d, J = 8.4 Hz, 2H), 7.70 (s, 4H), 7.64 (d, J = 8.4 Hz, 2H), 7.40−7.27 (m, 5H), 4.51 (s, 1H), 3.57 (s, 2H), 2.73−2.48 (m, 4H), 2.13−2.03 (m, J = 16.4 Hz, 2H), 1.98−1.87 (m, 2H). ^{13}C NMR (101 MHz, $CDCl_3$) δ 154.9, 143.5, 141.9, 138.3, 129.0, 128.3, 127.5, 127.4, 127.1, 126.9, 125.8, 125.8, 125.7, 96.3, 62.7, 50.5, 36.6. HRMS (ESI-TOF$^+$) m/z $[M+H]^+$ calcd for $C_{26}H_{25}F_3N_3O$: 452.1950, found: 452.1947.

*4.2.1.31. 8-Benzyl-3-(4-(thiophen-2-yl)phenyl)-1-oxa-2,4,8-triazaspiro[4.5]dec-2-ene (**A31**).* Yellow powder. Yield: 33.3%. Mp: 215−216 °C. ^{1}H NMR (400 MHz, $CDCl_3$) δ 7.71 (d, J = 8.3 Hz, 2H), 7.62 (d, J = 8.3 Hz, 2H), 7.51 (s, 1H), 7.40 (s, 2H), 7.44−7.24 (m, 5H), 4.56 (s, 1H), 3.57 (s, 2H), 2.78−2.51 (m, 4H), 2.10−2.03 (m, 2H), 1.94−1.86 (m, 2H). ^{13}C NMR (101 MHz, $CDCl_3$) δ 155.1, 141.2, 138.3, 138.0, 129.0, 128.2, 127.1, 126.8, 126.6, 126.5, 126.0, 124.5, 121.2, 109.9, 96.1, 62.7, 50.5, 36.6. HRMS (ESI-TOF$^+$) m/z $[M+H]^+$ calcd for $C_{23}H_{24}N_3OS$: 390.1640, found: 390.1631.

*4.2.1.32. 8-Benzyl-3-(4-(pyridin-3-yl)phenyl)-1-oxa-2,4,8-triazaspiro[4.5]dec-2-ene (**A32**).* Yellow powder. Yield: 99%. Mp: 173−174 °C. ^{1}H NMR (400 MHz, $CDCl_3$) δ 8.79 (s, 1H), 8.59 (d, J = 4.4 Hz, 1H), 7.85 (d, J = 8.0 Hz, 1H), 7.79 (d, J = 8.2 Hz, 2H), 7.57 (d, J = 8.1 Hz, 2H), 7.43−7.26 (m, 6H), 5.13 (s, 1H), 3.55 (s, 2H), 2.67−2.53 (m, 4H), 2.11−2.01 (m, 2H), 1.97−1.85 (m, 2H). ^{13}C NMR (101 MHz, $CDCl_3$) δ 155.0, 148.9, 148.1, 139.8, 138.3, 135.6, 134.3, 129.0, 128.2, 127.2, 127.1, 127.1, 125.8, 123.7, 96.3, 62.7, 50.5, 36.6. HRMS (ESI-TOF$^+$) m/z $[M+H]^+$ calcd for $C_{24}H_{25}N_4O$: 385.2028, found: 385.2027.

*4.2.1.33. 8-Benzyl-3-(4-(pyridin-4-yl)phenyl)-1-oxa-2,4,8-triazaspiro[4.5]dec-2-ene (**A33**).* Yellow powder. Yield: 86%. Mp: 211−212 °C. ^{1}H NMR (400 MHz, $CDCl_3$) δ 8.65 (d, J = 5.8 Hz, 2H), 7.80 (d, J = 8.3 Hz, 2H), 7.64 (d, J = 8.3 Hz, 2H), 7.48 (d, J = 6.0 Hz, 2H), 7.32 (d, J = 4.5 Hz, 5H), 5.05 (s, 1H), 3.55 (s, 2H), 2.73−2.43 (m, 4H),

2.14–1.99 (m, 2H), 1.97–1.83 (m, 2H). ^{13}C NMR (101 MHz, $CDCl_3$) δ 154.9, 150.3, 147.2, 140.1, 138.3, 129.0, 128.2, 127.2, 127.1126.7, 121.6, 121.5, 96.5, 62.7, 50.5, 36.6. HRMS (ESI-TOF$^+$) m/z [M+H]$^+$ calcd for $C_{24}H_{25}N_4O$: 385.2028, found: 385.2022.

*4.2.1.34. 8-Benzyl-3-(4-(2-methoxypyridin-4-yl)phenyl)-1-oxa-2,4,8-triazaspiro[4.5]dec-2-ene (**A34**).* White powder. Yield: 37.5%. Mp: 198–199 °C. ^{1}H NMR (400 MHz, $CDCl_3$) δ 8.23 (d, J = 5.2 Hz, 1H), 7.78 (d, J = 8.4 Hz, 2H), 7.65 (d, J = 8.4 Hz, 2H), 7.39–7.27 (m, 5H), 7.10 (d, J = 5.6 Hz, 1H), 6.95 (s, 1H), 4.45 (s, 1H), 3.99 (s, 3H), 3.58 (s, 2H), 2.72–2.55 (m, 4H), 2.12–2.05 (m, 2H), 1.95–1.85 (m, 2H). ^{13}C NMR (101 MHz, $CDCl_3$) δ 164.9, 154.8, 149.9, 147.4, 140.4, 138.0, 129.0, 128.3, 127.2, 127.1, 126.9, 115.1, 108.5, 96.3, 62.6, 53.6, 50.5, 36.6, 14.1. HRMS (ESI-TOF$^+$) m/z [M+H]$^+$ calcd for $C_{25}H_{27}N_4O_2$: 415.2134, found: 415.2130.

*4.2.1.35. 8-Benzyl-3-(6-(3-methoxyphenyl)pyridin-3-yl)-1-oxa-2,4,8-triazaspiro[4.5]dec-2-ene (**A35**).* White powder. Yield: 97.5%. Mp: 148–149 °C. ^{1}H NMR (400 MHz, $CDCl_3$) δ 8.92 (s, 1H), 8.05 (s, 1H), 7.76 (s, 1H), 7.70–7.29 (m, 8H), 6.99 (s, 1H), 4.69 (s, 1H), 3.89 (s, 3H), 3.57 (s, 2H), 2.91–2.41 (m, 4H), 2.15–2.02 (m, 2H), 1.97–1.89 (m, 2H). ^{13}C NMR (101 MHz, $CDCl_3$) δ 160.1, 158.9, 153.2, 147.1, 139.7, 138.2, 134.5, 129.9, 129.1, 128.3, 127.1, 120.6, 120.3, 119.4, 115.7, 112.1, 96.6, 62.6, 55.4, 50.4, 36.5. HRMS (ESI-TOF$^+$) m/z [M+H]$^+$ calcd for $C_{25}H_{27}N_4O_2$: 415.2134, found: 415.2129.

*4.2.1.36. 3-(5-(8-Benzyl-1-oxa-2,4,8-triazaspiro[4.5]dec-2-en-3-yl) pyridin-2-yl)aniline (**A36**).* White powder. Yield: 32.3%. Mp:173–174 °C. ^{1}H NMR (400 MHz, $CDCl_3$) δ 8.91 (s, 1H), 8.03 (d, J = 10.6 Hz, 1H), 7.73 (d, J = 8.3 Hz, 1H), 7.40 (s, 1H), 7.36–7.26 (m, 7H), 6.77 (d, J = 7.1 Hz, 1H), 4.55 (s, 1H), 3.80 (s, 2H), 3.57 (s, 2H), 2.82–2.43 (m, 4H), 2.14–2.00 (m, 2H), 1.98–1.86 (m, 2H). ^{13}C NMR (101 MHz, $CDCl_3$) δ 159.3, 153.2, 147.0, 147.0,139.4, 138.3, 134.4, 129.8, 129.0, 128.3, 127.1, 120.4, 120.2, 117.3, 116.4, 113.5, 96.6, 62.6, 50.5, 36.6. HRMS (ESI-TOF$^+$) m/z [M+H]$^+$ calcd for $C_{24}H_{26}N_5O$: 400.2137, found: 400.2132.

*4.2.2. General procedure for the synthesis of compounds **B1**–**B15***

A mixture of piperidin-4-one (104 mg, 1.05 mmol), **3a, 3b** (1 mmol) and Na_2CO_3 (318 mg, 3 mmol) in CH_3CN (3 mL) was stirred at room temperature for 45 min, followed by stirred at 50 °C for 45 min, then heated to 70 °C for an additional 2–10 h. After completion, the solvent was evaporated under reduced pressure. The residue was dissolved in EtOAc and washed with water three times, dried over anhydrous Na_2SO_4, filtered and concentrated under reduced pressure. The crude product was purfied by silica gel column chromatography eluting with DCM/MeOH (100/1) to afford **4a, 4b**.

TsOH•H_2O (37.5 mg, 0.2 mmol) was added to a solution of **2a, 2f, 2i, 2l** or **2m** (1 mmol) and **4a, 4b** or commercially available piperidones **4c-4e** (1.5 mmol) in toluene (5 mL). The mixture was refluxed overnight. After completion, the mixture was extracted with EtOAc three times. The combined organic layers were washed with brine, dried over anhydrous Na_2SO_4, filtered and concentrated under reduced pressure. The crude product was purified by silica gel column chromatography eluting with DCM/MeOH/NH_3•H_2O (100/3/1) to afford **B1**–**B12**.

$Pd(PPh_3)_4$ (113 mg, 0.1 mmol) was added to a degassed mixture of **B10** or **B12** (1 mmol), substituted boric acids (2 mmol), K_2CO_3 (483 mg, 3.5 mmol) in dioxane (4 mL) and water (2 mL) under argon. The mixture was heated at 80–120 °C for 6–20 h, cooled to room temperature and extracted with EtOAc three times. The combined organic layers were washed with brine, dried over anhydrous Na_2SO_4, filtered and concentrated under reduced pressure. The crude product was purified by silica gel column chromatography eluting with PE/EtOAc/TEA (20/10/1) to afford **B13**–**B15**.

*4.2.2.1. tert-Butyl 3-phenyl-1-oxa-2,4,8-triazaspiro[4.5]dec-2-ene-8-carboxylate (**B1**).* White powder. Yield: 87.8%. ^{1}H NMR (400 MHz, $CDCl_3$) δ 7.65 (d, J = 7.6 Hz, 2H), 7.49–7.39 (m, 1H), 7.38–7.28 (m, 2H), 5.11 (s, 1H), 3.97–3.68 (m, 2H), 3.41–3.16 (m, 2H), 2.07–1.86 (m, 2H), 1.85–1.68 (m, 2H), 1.44 (s, 9H). ^{13}C NMR (101 MHz, $CDCl_3$) δ 155.5, 154.6, 130.8, 128.6, 126.4, 125.6, 95.8, 79.8, 77.2, 41.2, 36.3, 28.4. HRMS (ESI-TOF$^+$) m/z [M+H]$^+$ calcd for $C_{17}H_{24}N_3O_3$: 318.1818, found: 318.1817.

*4.2.2.2. Ethyl 3-phenyl-1-oxa-2,4,8-triazaspiro[4.5]dec-2-ene-8-carboxylate (**B2**).* White powder. Yield: 44.1%. mp: 184–185 °C. ^{1}H NMR (400 MHz, $CDCl_3$) δ 7.68 (d, J = 7.8 Hz, 2H), 7.53–7.34 (m, 3H), 4.55 (brs, 1H), 4.15 (q, J = 7.2 Hz, 2H), 4.01–3.82 (m, 2H), 3.39 (t, J = 11.6 Hz, 2H), 2.17–1.97 (m, 2H), 1.87–1.68 (m, 2H), 1.27 (t, J = 7.2 Hz, 3H). ^{13}C NMR (101 MHz, $CDCl_3$) δ 155.4, 130.9, 128.7, 126.3, 125.6, 95.6, 61.5, 41.0, 36.3, 14.6. HRMS (ESI-TOF$^+$) m/z [M+H]$^+$ calcd for $C_{15}H_{20}N_3O_3$: 290.1505, found: 290.1507.

*4.2.2.3. Ethyl 3-(4-bromophenyl)-1-oxa-2,4,8-triazaspiro[4.5]dec-2-ene-8-carboxylate (**B3**).* White powder. Yield: 87.8% yield. Mp: 214–215 °C. ^{1}H NMR (400 MHz, $CDCl_3$) δ 7.55 (s, 4H), 4.44 (s, 1H), 4.15 (q, J = 7.0 Hz, 2H), 3.99–3.86 (m, 2H), 3.39 (t, J = 12.8 Hz, 2H), 2.09–1.98 (d, J = 12.8 Hz, 2H), 1.83–1.72 (m, 2H), 1.27 (t, J = 7.2 Hz, H). ^{13}C NMR (101 MHz, $CDCl_3$) δ 155.3, 154.7, 132.0, 127.8, 125.2, 124.6, 96.0, 61.5, 41.0, 36.3, 14.6. HRMS (ESI-TOF$^+$) m/z [M+H]$^+$ calcd for $C_{15}H_{19}BrN_3O_3$: 368.0611, found: 368.0611.

*4.2.2.4. 3-Phenyl-8-(pyridin-2-ylmethyl)-1-oxa-2,4,8-triazaspiro [4.5]dec-2-ene (**B4**).* Yellow powder. Yield: 49.3%. ^{1}H NMR (400 MHz, $CDCl_3$) δ 8.67 (d, J = 4.8 Hz, 1H), 8.03 (t, J = 7.8 Hz, 1H), 7.70–7.62 (m, 2H), 7.62–7.57 (m, 1H), 7.50 (d, J = 7.8 Hz, 1H), 7.47–7.36 (m, 3H), 5.17 (s, 1H), 4.05 (s, 2H), 3.36–3.23 (m, 2H), 2.99 − 2-82 (m, 2H), 2.66–2.49 (m, 2H), 2.23–2.17 (m, 2H). ^{13}C NMR (101 MHz, $CDCl_3$) δ 158.5, 155.4, 149.3, 136.4, 130.6, 128.6, 126.3, 125.9, 123.1, 122.0, 95.9, 64.2, 50.8, 36.5. HRMS (ESI-TOF$^+$) m/z [M+H]$^+$ calcd for $C_{18}H_{21}N_4O$: 309.1715, found: 309.1717.

*4.2.2.5. 8-(Pyridin-2-ylmethyl)-3-(thiazol-2-yl)-1-oxa-2,4,8-triazaspiro[4.5]dec-2-ene (**B5**).* Yellow powder. Yield: 30.1%. Mp: 148–149 °C. ^{1}H NMR (400 MHz, $CDCl_3$) δ 8.55 (d, J = 3.6 Hz, 1H), 7.84 (d, J = 2.8 Hz, 1H), 7.64 (t, J = 7.2 Hz, 1H), 7.51–7.31 (m, 2H), 7.23–7.01 (m, 1H), 5.53 (s, 1H), 3.68 (s, 2H), 2.91–2.53 (m, 4H), 2.21–2.00 (m, 2H), 2.00–1.85 (m, 2H). ^{13}C NMR (101 MHz, $CDCl_3$) δ 158.4, 153.5, 151.6, 149.3, 143.1, 136.4, 123.1, 122.0, 121.7, 97.6, 64.1, 50.6, 36.4. HRMS (ESI-TOF$^+$) m/z [M+H]$^+$ calcd for $C_{15}H_{18}N_5OS$: 316.1232, found: 316.1234.

*4.2.2.6. 3-(Isoquinolin-3-yl)-8-(pyridin-2-ylmethyl)-1-oxa-2,4,8-triazaspiro[4.5]dec-2-ene (**B6**).* Yellow powder. Yield: 42.1%. Mp: 184–185 °C. ^{1}H NMR (400 MHz, $CDCl_3$) δ 9.17 (s, 1H), 8.57 (d, J = 4.2 Hz, 1H), 8.35 (s, 1H), 7.97 (d, J = 8.2 Hz, 1H), 7.86 (d, J = 8.2 Hz, 1H), 7.72 (t, J = 7.2 Hz, 1H), 7.64 (t, J = 7.8 Hz, 2H), 7.39 (d, J = 7.8 Hz, 1H), 7.18–7.10 (m, 1H), 5.80 (s, 1H), 3.71 (s, 2H), 2.75–2.64 (m, 4H), 2.17–2.08 (m, 2H), 2.03–1.97 (m, 2H). ^{13}C NMR (101 MHz, $CDCl_3$) δ 158.6, 155.8, 151.9, 149.3, 138.5, 136.4, 135.6, 131.1, 129.0, 128.5, 127.6, 127.3, 123.1, 122.0, 119.1, 96.4, 64.2, 50.8, 36.5. HRMS (ESI-TOF$^+$) m/z [M+H]$^+$ calcd for $C_{21}H_{22}N_5O$: 360.1824, found: 360.1821.

*4.2.2.7. 8-(Pyridin-4-ylmethyl)-3-(thiazol-2-yl)-1-oxa-2,4,8-triazaspiro[4.5]dec-2-ene (**B7**).* Yellow powder. Yield: 19.7%. Mp: 231–232 °C. ^{1}H NMR (400 MHz, $CDCl_3$) δ 8.55 (d, J = 5.6 Hz, 2H), 7.87 (d, J = 3.2 Hz, 1H), 7.46 (d, J = 3.2 Hz, 1H), 7.28 (d, J = 2.8 Hz,

2H), 5.40 (s, 1H), 3.55 (s, 2H), 2.71–2.53 (m, 4H), 2.15–2.04 (m, 2H), 2.01–1.88 (m, 2H). ^{13}C NMR (101 MHz, $CDCl_3$) δ 153.4, 151.6, 149.8, 147.6, 143.2, 123.6, 121.8, 97.4, 61.3, 50.5, 36.4. HRMS (ESI-TOF$^+$) *m/z* $[M+H]^+$ calcd for $C_{15}H_{18}N_5OS$: 316.1232, found: 316.1231.

*4.2.2.8. 3-(Isoquinolin-3-yl)-8-(pyridin-4-ylmethyl)-1-oxa-2,4,8-triazaspiro[4.5]dec-2-en (**B8**).* Yellow powder. Yield: 50.1%. Mp: 157–158 °C. ^{1}H NMR (400 MHz, $CDCl_3$) δ 9.20 (s, 1H), 8.55 (d, *J* = 5.6 Hz, 2H), 8.37 (s, 1H), 8.00 (d, *J* = 8.0 Hz, 1H), 7.90 (d, *J* = 8.2 Hz, 1H), 7.75 (t, *J* = 8.0 Hz, 1H), 7.67 (t, *J* = 7.6 Hz, 1H), 7.30 (d, *J* = 5.8 Hz, 2H), 5.76 (s, 1H), 3.57 (s, 2H), 2.69–2.57 (m, 4H), 2.17–2.12 (m, 2H), 2.00–1.88 (m, 2H). ^{13}C NMR (101 MHz, $CDCl_3$) δ 155.9, 151.9, 149.8, 147.8, 138.4, 135.6, 131.1, 129.1, 128.5, 127.6, 127.4, 123.7119.1, 96.2, 61.4, 50.7, 36.5. HRMS (ESI-TOF$^+$) *m/z* $[M+H]^+$ calcd for $C_{21}H_{22}N_5O$: 360.1824, found: 360.1826.

*4.2.2.9. 8-Methyl-3-phenyl-1-oxa-2,4,8-triazaspiro[4.5]dec-2-ene (**B9**).* Yellow powder. Yield: 39.0%. Mp: 177–178 °C. ^{1}H NMR (400 MHz, $CDCl_3$) δ 7.68 (d, *J* = 6.8 Hz, 2H), 7.52–7.34 (m, 3H), 4.55 (s, 1H), 2.79–2.56 (m, 4H), 2.37 (s, 3H), 2.14–2.08 (m, 2H), 2.02–1.93 (m, 2H). ^{13}C NMR (101 MHz, $CDCl_3$) δ 155.3, 130.8, 128.7, 126.3, 125.8, 95.2, 52.7, 45.7, 36.3. HRMS (ESI-TOF$^+$) *m/z* $[M+H]^+$ calcd for $C_{13}H_{18}N_3O$: 232.1450, found: 232.1447.

*4.2.2.10. 3-(4-Bromophenyl)-8-methyl-1-oxa-2,4,8-triazaspiro[4.5]dec-2-ene (**B10**).* Yellow powder. Yield: 53.3%. mp: 230–231 °C. ^{1}H NMR (400 MHz, $CDCl_3$) δ 7.65–7.35 (m, 4H), 5.13 (s, 1H), 2.92–2.57 (m, 4H), 2.41 (s, 3H), 2.14–1.96 (m, 4H). ^{13}C NMR (101 MHz, $CDCl_3$) δ 154.8, 131.8, 127.9, 125.0, 124.7, 95.2, 52.6, 45.5, 35.8. HRMS (ESI-TOF$^+$) *m/z* $[M+H]^+$ calcd for $C_{13}H_{17}BrN_3O$: 310.0555, found: 310.0554.

*4.2.2.11. 8-Methyl-3-(thiazol-2-yl)-1-oxa-2,4,8-triazaspiro[4.5]dec-2-ene (**B11**).* Yellow powder. Yield: 37.1%. Mp: 182–183 °C. ^{1}H NMR (400 MHz, $CDCl_3$) δ 7.86 (s, 1H), 7.46 (s, 1H), 5.52 (s, 1H), 3.03–2.48 (m, 4H), 2.35 (s, 3H), 2.16–2.04 (m, 2H), 2.04–1.92 (m, 2H). ^{13}C NMR (101 MHz, $CDCl_3$) δ 153.3, 151.6, 143.2, 121.8, 96.9, 52.6, 45.6, 36.1. HRMS (ESI-TOF$^+$) *m/z* $[M+H]^+$ calcd for $C_{10}H_{15}N_4OS$: 239.0967, found: 239.0967.

*4.2.2.12. 3-(6-Bromopyridin-3-yl)-8-methyl-1-oxa-2,4,8-triazaspiro[4.5]dec-2-ene (**B12**).* White powder. Yield: 17.2%. mp: 176–177 °C. ^{1}H NMR (400 MHz, DMSO-d_6) δ 8.66 (s, 1H), 7.98 (d, *J* = 8.4 Hz, 1H), 7.78 (d, *J* = 8.4 Hz, 2H), 2.73–2.57 (m, 2H), 2.48–2.36 (m, 2H), 2.27 (s, 3H), 1.89–1.76 (m, 4H). ^{13}C NMR (101 MHz, DMSO-d_6) δ 152.6, 148.0, 143.3, 137.0, 128.7, 122.3, 96.2, 52.3, 45.6, 36.0. HRMS (ESI-TOF$^+$) *m/z* $[M+H]^+$ calcd for $C_{12}H_{16}N_4OBr$: 311.0507, found: 311.0508.

*4.2.2.13. 3-(3′-methoxy-[1,1′-biphenyl]-4-yl)-8-methyl-1-oxa-2,4,8-triazaspiro[4.5]dec-2-ene (**B13**).* Yellow powder. Yield: 66.7% yield. Mp: 225–226 °C. ^{1}H NMR (400 MHz, DMSO-d_6) δ 7.83–7.70 (m, 4H), 7.53 (s, 1H), 7.43–7.36 (m, 1H), 7.32–7.26 (m, 1H), 7.26–7.22 (m, 1H), 6.97 (dd, *J* = 8.2, 2.4 Hz, 1H), 3.83 (s, 3H), 2.78–2.59 (m, 2H), 2.47–2.32 (m, 2H), 2.29 (s, 3H), 1.92–1.76 (m, 4H). ^{13}C NMR (101 MHz, DMSO-d_6) δ 160.2, 155.0, 142.2, 141.0, 130.5, 127.3, 127.1, 125.4, 119.4, 114.0, 112.6, 95.3, 57.7, 55.6, 52.4, 36.0. HRMS (ESI-TOF$^+$) *m/z* $[M+H]^+$ calcd for $C_{20}H_{24}N_3O_2$: 338.1869, found: 338.1868.

*4.2.2.14. 4′-(8-methyl-1-oxa-2,4,8-triazaspiro[4.5]dec-2-en-3-yl)-[1,1′-biphenyl]-3-amine (**B14**).* Brown solid. Yield: 77.8%. Mp: 225–226 °C. ^{1}H NMR (400 MHz, $CDCl_3$) δ 7.71 (d, *J* = 8.2 Hz, 2H), 7.58 (d, *J* = 8.2 Hz, 2H), 7.22 (t, *J* = 7.8 Hz, 1H), 6.97 (d, *J* = 7.6 Hz, 1H), 6.89 (s, 1H), 6.70 (d, *J* = 7.8 Hz, 1H), 4.76 (s, 1H), 3.74 (brs, 2H), 2.70–2.56 (m, 4H), 2.37 (s, 3H), 2.13–2.03 (m, 2H), 1.99–1.92 (m, 2H). ^{13}C NMR (101 MHz, $CDCl_3$) δ 155.3, 146.9, 143.7, 141.1, 129.8, 127.2, 126.7, 124.5, 117.4, 114.7, 113.6, 95.3, 52.7, 45.8, 36.3. HRMS (ESI-TOF$^+$) *m/z* $[M+H]^+$ calcd for $C_{19}H_{23}N_4O$: 323.1872, found: 323.1869.

*4.2.2.15. 3-(4-(2-Methoxypyridin-4-yl)phenyl)-8-methyl-1-oxa-2,4,8-triazaspiro[4.5]dec-2-ene (**B15**).* Yellow powder. Yield: 50.0%. Mp: 225–226 °C. ^{1}H NMR (400 MHz, DMSO-d_6) δ 8.25 (d, *J* = 5.4 Hz, 1H), 7.89 (d, *J* = 8.4 Hz, 2H), 7.80 (d, *J* = 8.4 Hz, 2H), 7.72 (s, 1H), 7.35 (d, *J* = 6.6 Hz, 1H), 7.16 (s, 1H), 3.90 (s, 3H), 2.97–2.79 (m, 2H), 2.75–2.55 (m, 2H), 2.41 (s, 3H), 2.04–1.83 (m, 4H). ^{13}C NMR (101 MHz, DMSO-d_6) δ 164.9, 154.9, 149.6, 148.0, 139.2, 127.5, 127.2, 126.9, 115.4, 108.0, 95.0, 55.3, 53.7, 52.0, 35.3. HRMS (ESI-TOF$^+$) *m/z* $[M+H]^+$ calcd for C19H23N4O2: 339.1820, found: 339.1821.

4.3. TEVC recording in xenopus oocytes

Similar to our previously reported protocol [39,40], oocytes were harvested from *Xenopus* laevis female clawed frogs after anesthesia, and washed twice in the Ca^{2+}-free OR2 solution (82.5 mM NaCl, 2.5 mM KCl, 1 mM $MgCl_2$, 5 mM HEPES, pH 7.4) before transferred to ~25-mL tubes. Oocytes were then treated with 2 mg/mL collagenase in OR2 solution (Sigma type II, Sigma-Aldrich Inc, St Louis, MO, USA) for 20 min at room temperature under gentle rotation. The stage V and VI oocytes were selected for microinjections. For TEVC recordings in oocytes, capped cRNAs were transcribed *in vitro* using the T3 mMESSAGEmMACHINE Kit (Ambion, Austin, TX, USA) following the linearization of plasmids in pBluescript KSM vectors. The oocytes were injected with 46 nL of cRNA solution containing approximately 20 ng human α7 nAChR cRNA using a micro-injector (Drummond Scientific, Broomall, PA, USA). For the expression of heteromeric rat α3β4 and rat α4β2 nAChRs, approximately total of 2 ng cRNAs were injected in a 1:1 combination of each subunit into oocytes that were incubated at 16 °C in ND96 solution (96 mM NaCl, 2 mM KCl, 1.8 mM $CaCl_2$, 1 mM $MgCl_2$, 5 mM 4-(2-hydroxyethyl)1-piperazineethanesulphonic acid (HEPES), pH 7.4 adjusted with NaOH). Recordings were made 24–72 h post-injections. Oocytes were impaled with two microelectrodes (0.5–1.0 MΩ) filled with 3 M KCl in a 40-μL recording chamber. The membrane potential was held at −90 mV using standard voltage clamp procedures. Currents were recorded in Ringer's solution (115 mM NaCl, 2.5 mM KCl, 10 mM HEPES, 1.8 mM $CaCl_2$, 1 mM $MgCl_2$, 0.0005 mM atropine) at room temperature (22 ± 1 °C) using a GeneClamp 500B amplifier (Axon Instruments, Union City, CA, USA).

4.4. Data analysis

All data were expressed as the means ± SEM. Statistical significance was assessed by Student's t-test and one-way ANOVA using the Prism version 5.0 software. $P < 0.05$ was considered statistically significant. In the TEVC recordings, currents were quantified by measuring peak current amplitudes and analyzed using PatchMaster and Origin 9.0 software. The concentration–response curves were fitted to the Hill equation as follows: $I_{normalized} = 1-1/(1 + (IC_{50}/C)n_H)$.

4.5. Virtual screening

4.5.1. Preparation of compound library

In brief, ChemDiv database was prepared by a homemade protocol in Pipeline Pilot v7.5 (PP 7.5, Accelrys, Inc.), in which the molecules formed 3D coordinates. The prepared database was filtered by a basic standard in FILTER (OpenEye Scientific Software,

Inc) to eliminate molecules with unsatisfied properties according to "rule of five". Subsequently, the database was prepared with OMEGA (OpenEye Scientific Software, Inc) to generate up to 500 conformations for each molecule.

4.5.2. Pharmacophore-based search

For the pharmacophore generation, 3D structures of training set (11 selected compounds) were generated and energy minimized by using LigPrep module of Schrödinger Suite (Schrödinger, LLC, New York, NY, USA). Optimized conformations of training set were submitted to the common feature pharmacophore generation procedure in Discovery Studio 2.5 (DS 2.5, Accelrys, Inc.). The HipHop module in Catalyst was used to identify and overlay common features shared by the training set. The MaxOmitFeat of all compounds in training set were set to 1, and the Principal of compound nicotine and Epibatidine were set to 0, compound TC-1698 and 7aa were set to 1, other compounds were set to 2. Hydrogen bonding acceptor, Hydrogen bonding doner, POS Charge, PosIonizable and Hydrophobic, were selected as pharmocophoric features based on the chemical features present in the training set. The Minimum features were set to 3, and the Minimum inter-feature distance was set to 1. According to the matching of the training set compounds, we selected the Hip06 model from the total 10 pharmacophores developed, which contained 1 hydrogen-bond receptor, 1 hydrophobic center and 1 positively ionized group. The HipHop model was used to search prepared ChemDiv database. The results were ranked by 'Fit Value' score and the top 10% compounds were retained.

The recursive partitioning (RP) model was constructed by E-state key and topological descriptors based on chemical graph theory in PP 7.5 [41]. The true positive 42 reported agonists were set as an active class, and the 999 decoy compounds from Schrödinger were selected as an inactive class. The ROC score of the RP model obtained in this study was 0.9964. HipHop output compounds were used as input for RP model, and the active class were retained. Finally, 13 compounds were selected and purchased from the commercial source for biological evaluation.

4.6. Docking studies

The molecular docking studies were carried out by using Induced Fit Docking module of Schrödinger Suite (Schrödinger, LLC, New York, NY, USA) [40]. Crystal structure of human α7-AChBP chimera (PDB ID code: 3SQ6) was chosen for docking studies. The protein was prepared using the protein preparation wizard, which assigned bond orders, added hydrogen atoms and removed water molecules. Then the protein was energy minimized by restrained minimization using OPLS3 force field. The grid was generated at orthosteric site, which was identified by picking out the original co-crystalized ligand using Receptor Grid Generation module. For the preparation of **T761**–**0184** and **B10**, 3D structures were generated and energy minimized by using LigPrep module. We used Induced Fit Docking module to dock **T761**–**0184** and **B10** with the orthosteric site of α7 AChR for more accurate binding conformation, and Glide XP was chosen for docking precision.

Declaration of competing interest

The authors declare that they have no known competing financial interests or personal relationships that could have appeared to influence the work reported in this paper.

Acknowledgments

This research was supported by the National Natural Science Foundation of China (81373272, 21772005, 81872730) and the Beijing Natural Science Foundation (7202088, 7172118). We are very appreciative of Dr. Wei Huang (Chinese Academy of Medical Sciences, Beijing) for their help in this work.

Appendix A. Supplementary data

Supplementary data to this article can be found online at https://doi.org/10.1016/j.ejmech.2020.112774.

References

[1] R. Hurst, H. Rollema, D. Bertrand, Nicotinic acetylcholine receptors: from basic science to therapeutics, Pharmacol. Ther. 137 (2013) 22–54.
[2] K. Kaczanowska, G.A. Camacho Hernandez, L. Bendiks, L. Kohs, J.M. Cornejo-Bravo, M. Harel, M.G. Finn, P. Taylor, Substituted 2-Aminopyrimidines selective for α7-nicotinic acetylcholine receptor activation and Association with acetylcholine binding proteins, J. Am. Chem. Soc. 139 (2017) 3676–3684.
[3] E. Cooper, S. Couturier, M. Ballivet, Pentameric structure and subunit stoichiometry of a neuronal nicotinic acetylcholine receptor, Nature 350 (1991) 235–238.
[4] R.J. Lukas, J.P. Changeux, N. Le Novère, E.X. Albuquerque, D.J. Balfour, D.K. Berg, D. Bertrand, V.A. Chiappinelli, P.B. Clarke, A.C. Collins, J.A. Dani, S.R. Grady, K.J. Kellar, J.M. Lindstrom, M.J. Marks, M. Quik, P.W. Taylor, S. Wonnacott, International Union of Pharmacology. XX. Current status of the nomenclature for nicotinic acetylcholine receptors and their subunits, Pharmacol. Rev. 51 (1999) 397–401.
[5] J. Lindstrom, R. Anand, V. Gerzanich, X. Peng, F. Wang, G. Wells, Structure and function of neuronal nicotinic acetylcholine receptors, Prog. Brain Res. 109 (1996) 125–137.
[6] L.F. Yu, H.K. Zhang, B.J. Caldarone, J.B. Eaton, R.J. Lukas, A.P. Kozikowski, Recent developments in novel antidepressants targeting α4β2-nicotinic acetylcholine receptors, J. Med. Chem. 57 (2014) 8204–8223.
[7] C. Bouzat, M. Lasala, B.E. Nielsen, J. Corradi, M.D.C. Esandi, Molecular function of α7 nicotinic receptors as drug targets, J. Physiol. 596 (2018) 1847–1861.
[8] B. Lendvai, F. Kassai, A. Szájli, Z. Némethy, α7 nicotinic acetylcholine receptors and their role in cognition, Brain Res. Bull. 93 (2013) 86–96.
[9] K.T. Dineley, A.A. Pandya, J.L. Yakel, Nicotinic ACh receptors as therapeutic targets in CNS disorders, Trends Pharmacol. Sci. 36 (2015) 96–108.
[10] J. Egea, I. Buendia, E. Parada, E. Navarro, R. León, M.G. Lopez, Anti-inflammatory role of microglial alpha7 nAChRs and its role in neuroprotection, Biochem. Pharmacol. 97 (2015) 463–472.
[11] M.L. Sinkus, S. Graw, R. Freedman, R.G. Ross, H.A. Lester, S. Leonard, The human CHRNA7 and CHRFAM7A genes: a review of the genetics, regulation, and function, Neuropharmacology 96 (2015) 274–288.
[12] P. Dasgupta, W. Rizwani, S. Pillai, R. Kinkade, M. Kovacs, S. Rastogi, S. Banerjee, M. Carless, E. Kim, D. Coppola, E. Haura, S. Chellappan, Nicotine induces cell proliferation, invasion and epithelial-mesenchymal transition in a variety of human cancer cell lines, Int. J. Canc. 124 (2009) 36–45.
[13] C.H. Wu, C.H. Lee, Y.S. Ho, Nicotinic acetylcholine receptor-based blockade: applications of molecular targets for cancer therapy, Clin. Canc. Res. : an official journal of the American Association for Cancer Research 17 (2011) 3533–3541.
[14] C. Pepper, H. Tu, P. Morrill, S. Garcia-Rates, C. Fegan, S. Greenfield, Tumor cell migration is inhibited by a novel therapeutic strategy antagonizing the alpha-7 receptor, Oncotarget 8 (2017) 11414–11424.
[15] R.D. Sheridan, A.P. Smith, S.R. Turner, J.E. Tattersall, Nicotinic antagonists in the treatment of nerve agent intoxication, J. R. Soc. Med. 98 (2005) 114–115.
[16] N. Walker, C. Howe, M. Glover, H. McRobbie, J. Barnes, V. Nosa, V. Parag, B. Bassett, C. Bullen, Cytisine versus nicotine for smoking cessation, N. Engl. J. Med. 371 (2014) 2353–2362.
[17] C. Stokes, M. Treinin, R.L. Papke, Looking below the surface of nicotinic acetylcholine receptors, Trends Pharmacol. Sci. 36 (2015) 514–523.
[18] K. Brejc, W.J. van Dijk, R.V. Klaassen, M. Schuurmans, J. van Der Oost, A.B. Smit, T.K. Sixma, Crystal structure of an ACh-binding protein reveals the ligand-binding domain of nicotinic receptors, Nature 411 (2001) 269–276.
[19] C.M. de Fiebre, E.M. Meyer, J.C. Henry, S.I. Muraskin, W.R. Kem, R.L. Papke, Characterization of a series of anabaseine-derived compounds reveals that the 3-(4)-dimethylaminocinnamylidine derivative is a selective agonist at neuronal nicotinic alpha 7/125I-alpha-bungarotoxin receptor subtypes, Mol. Pharmacol. 47 (1995) 164–171.
[20] A.A. Jensen, B. Frølund, T. Liljefors, P. Krogsgaard-Larsen, Neuronal nicotinic acetylcholine receptors: structural revelations, target identifications, and therapeutic inspirations, J. Med. Chem. 48 (2005) 4705–4745.
[21] D. Feuerbach, J. Nozulak, K. Lingenhoehl, K. McAllister, D. Hoyer, JN403, in vitro characterization of a novel nicotinic acetylcholine receptor alpha7 selective agonist, Neurosci. Lett. 416 (2007) 61–65.
[22] P. Pichat, O.E. Bergis, J.P. Terranova, A. Urani, C. Duarte, V. Santucci, C. Gueudet, C. Voltz, R. Steinberg, J. Stemmelin, F. Oury-Donat, P. Avenet, G. Griebel, B. Scatton, SSR180711, a Novel Selective Alpha7 Nicotinic Receptor Partial Agonist: (II) Efficacy in Experimental Models Predictive of Activity

against Cognitive Symptoms of Schizophrenia vol. 32, official publication of the American College of Neuropsychopharmacology, Neuropsychopharmacology, 2007, pp. 17–34.
[23] T.L. Wallace, P.M. Callahan, A. Tehim, D. Bertrand, G. Tombaugh, S. Wang, W. Xie, W.B. Rowe, V. Ong, E. Graham, A.V. Terry Jr., J.S. Rodefer, B. Herbert, M. Murray, R. Porter, L. Santarelli, D.A. Lowe, RG3487, a novel nicotinic α7 receptor partial agonist, improves cognition and sensorimotor gating in rodents, J. Pharmacol. Exp. Therapeut. 336 (2011) 242–253.
[24] D. Feuerbach, N. Pezous, M. Weiss, K. Shakeri-Nejad, K. Lingenhoehl, D. Hoyer, K. Hurth, G. Bilbe, C.R. Pryce, K. McAllister, F. Chaperon, K. Kucher, D. Johns, T. Blaettler, C. Lopez Lopez, AQW051, a novel, potent and selective α7 nicotinic ACh receptor partial agonist: pharmacological characterization and phase I evaluation, Br. J. Pharmacol. 172 (2015) 1292–1304.
[25] X. Xiu, N.L. Puskar, J.A. Shanata, H.A. Lester, D.A. Dougherty, Nicotine binding to brain receptors requires a strong cation-pi interaction, Nature 458 (2009) 534–537.
[26] A.A. Mazurov, J.D. Speake, D. Yohannes, Discovery and development of α7 nicotinic acetylcholine receptor modulators, J. Med. Chem. 54 (2011) 7943–7961.
[27] D. Manetti, C. Bellucci, S. Dei, E. Teodori, K. Varani, E. Spirova, D. Kudryavtsev, I. Shelukhina, V. Tsetlin, M.N. Romanelli, New quinoline derivatives as nicotinic receptor modulators, Eur. J. Med. Chem. 110 (2016) 246–258.
[28] J.T. Kantrowitz, D.C. Javitt, R. Freedman, P. Sehatpour, L.S. Kegeles, M. Carlson, T. Sobeih, M.M. Wall, T.H. Choo, B. Vail, J. Grinband, J.A. Lieberman, Double Blind, Two Dose, Randomized, Placebo-Controlled, Cross-Over Clinical Trial of the Positive Allosteric Modulator at the Alpha7 Nicotinic Cholinergic Receptor AVL-3288 in Schizophrenia Patients vol. 45, official publication of the American College of Neuropsychopharmacology, Neuropsychopharmacology, 2020, pp. 1339–1345.
[29] Y. Peng, Q. Zhang, G.L. Snyder, H. Zhu, W. Yao, J. Tomesch, R.L. Papke, J.P. O'Callaghan, W.J. Welsh, L.P. Wennogle, Discovery of novel alpha7 nicotinic receptor antagonists, Bioorg. Med. Chem. Lett 20 (2010) 4825–4830.
[30] Y. Brissonnet, R. Araoz, R. Sousa, L. Percevault, S. Brument, D. Deniaud, D. Servent, J.Y. Le Questel, J. Lebreton, S.G. Gouin, Di- and heptavalent nicotinic analogues to interfere with α7 nicotinic acetylcholine receptors, Bioorg. Med. Chem. 27 (2019) 700–707.
[31] B. Sadek, A. Ashoor, A. Al Mansouri, D.E. Lorke, S.M. Nurulain, G. Petroianu, M. Wainwright, M. Oz, N3,N7-diaminophenothiazinium derivatives as antagonists of α7-nicotinic acetylcholine receptors expressed in Xenopus oocytes, Pharmacol. Res. 66 (2012) 213–218.
[32] D.R. Garton, S.G. Ross, R. Maldonado-Hernández, M. Quick, J.A. Lasalde-Dominicci, J.E. Lizardi-Ortiz, Amphetamine enantiomers inhibit homomeric α7 nicotinic receptor through a competitive mechanism and within the intoxication levels in humans, Neuropharmacology 144 (2019) 172–183.
[33] O. Dror, D. Schneidman-Duhovny, Y. Inbar, R. Nussinov, H.J. Wolfson, Novel approach for efficient pharmacophore-based virtual screening: method and applications, J. Chem. Inf. Model. 49 (2009) 2333–2343.
[34] C. Iwuagwu, D. King, I.M. McDonald, J. Cook, F.C. Zusi, M.D. Hill, R.A. Mate, H. Fang, R. Knox, L. Gallagher, D. Post-Munson Amy Easton, R. Miller, Y. Benitex, J. Siuciak, N. Lodge, R. Zaczek, D. Morgan, L. Bristow, J.E. Macor, R.E. Olson, Design and synthesis of a novel series of 4-heteroarylamino-1'-azaspiro[oxazole-5,3'-bicyclo[2.2.2]octanes as α7 nicotinic receptor agonists 2. Development of 4-heteroaryl SAR, Bioorg. Med. Chem. Lett 27 (2017) 1261–1266.
[35] S.X. Li, S. Huang, N. Bren, K. Noridomi, C.D. Dellisanti, S.M. Sine, L. Chen, Ligand-binding domain of an α7-nicotinic receptor chimera and its complex with agonist, Nat. Neurosci. 14 (2011) 1253–1259.
[36] M. Seki, O. Tsuruta, Y. Aoyama, A. Soejima, H. Shimada, H. Nonaka, Synthesis and pharmacological evaluation of 3-amino-1-(5-indanyloxy)-2-propanol derivatives as potent sodium channel blockers for the treatment of stroke, Chem. Pharm. Bull. 60 (2012) 488–498.
[37] H. Zhang, H. Liu, X. Luo, Y. Wang, Y. Liu, H. Jin, Z. Liu, W. Yang, P. Yu, L. Zhang, L. Zhang, Design, synthesis and biological activities of 2,3-dihydroquinazolin-4(1H)-one derivatives as TRPM2 inhibitors, Eur. J. Med. Chem. 152 (2018) 235–252.
[38] A. Taly, P.J. Corringer, D. Guedin, P. Lestage, J.P. Changeux, Nicotinic receptors: allosteric transitions and therapeutic targets in the nervous system, Nat. Rev. Drug Discov. 8 (2009) 733–750.
[39] Y. Xue, J. Tang, X. Ma, Q. Li, B. Xie, Y. Hao, H. Jin, K. Wang, G. Zhang, L. Zhang, L. Zhang, Synthesis and biological activities of indolizine derivatives as alpha-7 nAChR agonists, Eur. J. Med. Chem. 115 (2016) 94–108.
[40] Y. Xue, X. He, T. Yang, Y. Wang, Z. Liu, G. Zhang, Y. Wang, K. Wang, L. Zhang, L. Zhang, Discovery of fused heterocyclic carboxamide derivatives as novel α7-nAChR agonists: synthesis, preliminary SAR and biological evaluation, Eur. J. Med. Chem. 182 (2019) 111618.
[41] H.J. Kim, M.R. Doddareddy, H. Choo, Y.S. Cho, K.T. No, W.K. Park, A.N. Pae, New serotonin 5-HT(6) ligands from common feature pharmacophore hypotheses, J. Chem. Inf. Model. 48 (2008) 197–206.